ROLE OF TRANSCRIPTION FACTOR RUNX1 IN UTERINE STROMAL CELL DIFFERENTIATION AND MATERNAL-FETAL INTERACTION DURING MOUSE PREGNANCY

BY

KANNAN ATHILAKSHMI

THESIS

Submitted in partial fulfillment of the requirements
for the degree of Master of Science in VMS – Comparative Biosciences
in the Graduate College of the
University of Illinois at Urbana-Champaign, 2013

Urbana, Illinois

Adviser:

Professor Indrani C. Bagchi

ABSTRACT

The differentiation of endometrial stromal cells to decidual cells, a process known as decidualization, is essential for the establishment of pregnancy. The decidual tissue produces multitude of factors that control a variety of physiological processes at the fetal-maternal interface, such as endometrial vasculogenesis, modulation of maternal immune response, spiral artery modification and trophoblast invasion. An aberrant decidual response is associated with various pregnancy disorders, including spontaneous miscarriage, intrauterine growth restriction and preeclampsia. Our study revealed that the expression of Runx1, a transcription factor belonging to the runt-domain family, is markedly elevated in the uterine stromal cells during decidualization. Conditional deletion of the uterine *Runx1* gene led to severe embryo growth retardation and pregnancy loss during mid-gestation. Histological analysis of the *Runx1*-null uteri at gestation days 10-12 revealed an abnormally dense decidual tissue resulting from enhanced proliferation, impaired differentiation, and lack of apoptosis of stromal cells. The loss of *Runx1* expression in uterine stromal cells also resulted in a marked impairment in the development of maternal blood vessels concomitant with a marked down regulation of several angiogenic factors, such as VEGF-A and angiopoietin-2. Furthermore, immunohistochemical analysis of smooth muscle actin and cytokeratin in the uterine sections of the mutant mice revealed a lack of maternal spiral artery modification and restricted trophoblast invasion. Collectively, these studies demonstrated that in the absence of *Runx1* the decidua fails to produce critical factors that impact blood vessel formation, spiral artery modification, stromal apoptosis, and trophoblast migration. Thus, the *Runx1*-conditional knockout mouse presents an important animal model to study the molecular pathways that operate at the maternal-fetal interphase to control events that are critical for maintenance of pregnancy.

To three generation of women in my family,

My mother, sister, daughter and two nieces

whose unconditional love and exceptional support brought me this far

Acknowledgement

My profound gratitude to Dr. Indrani Bagchi for giving me the chance to work in her laboratory, encouragement, guidance, freedom and flexibility to carry out my work and her total support for me to pursue my master's degree. I am always indebted to Dr. Milan Bagchi for his continuous support, encouragement, and above all for believing in me. I have been extremely fortunate for their support throughout my stay in their laboratory and also providing us a healthy environment to carry out our work. I am immensely grateful for the opportunity they have provided me to learn and enjoy something new every day.

I would like to thank our collaborators, Dr.Gary Gilliland for providing us with Runx1 floxed mice, Dr. Fransesco DeMayo and Dr. John.P.Lydon for PR-Cre mice which were critical for my thesis work. I express my gratitude to my committee members, Dr. Jodi Flaws, Dr. Suzanne E.Berry-Miller and Dr. David Bunick and for their encouragement, support and valuable criticism throughout my study.

I take this opportunity to express my gratitude to my colleague and best friend Dr. Quanxi Li for all his assistance, criticism and especially his comradeship. We worked together in many projects and through discussions, arguments and hard work churned out exciting results. I would like to thank Dr. Shanmugasundaram Nallasamy for taking care of the mouse colony, without which my work would have been very difficult. My sincere thanks to Dr. Mary Laws, for all her support and friendship. My sincere appreciation for Juanmahel Davila whose passion for teaching and infectious enthusiasm made me learn so much without giving up. I also would like to thank all current and past Drs. Milan and Indrani Bagchi lab members for their continuous support. I also like to thank Dr. Jodi Flaws' lab members for their assistance.

I thank Karen Doty of Histology department for her histology work and helpful suggestions. I also would like to thank Ms. Carrol Bunick and all CB Department staff for all their help in keeping me on track with my degree requirements.

TABLE OF CONTENTS

CHAPTER 1 1

INTRODUCTION AND LITERATURE REVIEW 1

1.1 Introduction 1

1.2 Literature Review 2

1.2.1 Implantation 3

1.2.2 Decidualization 3

1.2.3 Angiogenesis 4

1.2.4 Placentation 4

1.2.5 Runx1- a member of Runx family of transcription factors 5

1.2.6 Runx genes and reproductive tissues 6

CHAPTER 2 8

MATERIALS AND METHODS 8

2.1 Animals and Tissue Collection 8

2.2 Histology 9

2.3 Immunohistochemistry/Immunofluorescence 10

2.4 Western blot analysis 10

2.5 Alkaline Phosphatase Activity 11

2.6 Quantitative real time PCR analysis (QPCR) 11

2.7 TUNEL & Dolichos Biflorus Agglutinin (DBA) staining 12

2.8 Statistical Analysis 12

2.9 Quantitation using ImageJ 13

CHAPTER 3 14

RESULTS 14

3.1 Estrogen induces *Runx1* expression in mouse uterus during early pregnancy 14

3.2 Spatio-temporal expression of *Runx1* during early pregnancy 15

3.3 Uterine ablation of *Runx1* leads to severe sub fertility 15

3.4 Ovarian function is unaffected in *Runx1*$^{d/d}$ female mice 16

3.5 Subfertility in *Runx1*$^{d/d}$ mice is due to a defect in uterine function 16

3.6 Histological analysis of mid pregnancy implantation sites 17
3.7 Deletion of *Runx1* leads to persistent stromal cell proliferation in the uterus 18
3.8 Impaired terminal differentiation of decidual cells in *Runx1*$^{d/d}$ uteri 19
3.9 *Runx1*$^{d/d}$ mice exhibit impaired angiogenesis during early pregnancy 19
3.10 Abnormal maternal vascular remodeling and impaired trophoblast invasion in *Runx1*$^{d/d}$ decidua during mid-pregnancy 20
CHAPTER 4 23
DISCUSSION 23
FIGURES AND TABLES 26
..... 26
REFERENCES 51

CHAPTER 1
INTRODUCTION AND LITERATURE REVIEW

1.1 Introduction

Steroid hormones, estrogen (E) and progesterone (P) critically regulate cell proliferation, differentiation, remodeling, and menstrual shedding of the endometrium. In each cycle, under the influence of these hormones, the endometrium becomes competent to receive the embryo during a short duration of time known as "window of receptivity". Embryo-uterine interactions leading to implantation and establishment of pregnancy occur during this period (1-3). About one third of human pregnancies end in spontaneous abortion and among these losses, 22% of them occur even before pregnancy is clinically detected. Implantation failure still remains an unsolved problem in reproductive medicine and it is the major cause of infertility.

In murine and human pregnancies, embryos implant by attaching to the luminal epithelium and invading into the stroma of the endometrium. In response to E and P, the stromal cells surrounding the implanting embryo undergo a remarkable transformation event. This process, known as decidualization, is an essential prerequisite for implantation (4-7). It involves morphogenetic, biochemical and vascular changes driven by the E and P receptors. The development of mutant mouse models lacking these receptors has firmly established the necessity of steroid signaling for decidualization. Genomic profiling of mouse and human endometrium has uncovered a complex, yet highly conserved network of steroid-regulated genes that supports decidualization. In order to advance our understanding of the mechanisms regulating implantation and better address the clinical challenges of infertility and endometrial diseases such as endometriosis, it is important to integrate the information gained from the mouse and human models (8-10).

1.2 Literature Review

Ovarian steroid hormones E and P act in concert to control uterine competency for embryo implantation (11-15). In mice, the attachment of the embryo to uterine epithelium occurs on day 4 of pregnancy. The attachment of the embryo to the uterine epithelium promotes the differentiation of the underlying fibroblastic stromal cells into morphologically distinct decidual cells, in a process termed as decidualization. Thus, transformed decidual cells have unique biosynthetic and secretory properties. They secrete hormones, growth factors and cytokines, essential for tissue and vascular remodeling to support the growth and development of the embryo. Undoubtedly these timely and orderly changes in the endometrium are critical events for maternal-fetal interactions leading to successful term pregnancy (16). In humans, implantation occurs 5-9 days after ovulation. While the decidual program in humans is initiated in the absence of the embryo, the extent of decidualization increases significantly with the onset of implantation and establishment of pregnancy (17). Perturbations in the decidual program may lead to pregnancy complications such as ectopic pregnancy, intra-uterine growth restriction, preeclampsia and thus, adversely influence fertility (7).

To understand the molecular basis of pregnancy complications in the human, functional studies employing transgenic mouse models are useful (18,19). Indeed studies over the past several years have yielded valuable information regarding the mechanisms that regulate implantation. This dissertation is focused on the role of transcription factor Runx1 in the regulation of decidualization and placentation during early pregnancy.

1.2.1 Implantation

Embryo – uterine interactions leading to implantation involves a series of complex interaction between the developing embryo and the uterus (20,21). Major events of the implantation process are synchronized development of the embryo to the blastocyst stage and a receptive uterus through steroid hormone dependent changes. Lack of this synchronization leads to implantation failure. In mice, there is a transitory rise in Estrogen on day 4 of pregnancy known as "nidatory estrogen" which is responsible for implantation. Steroid hormones also regulate these processes in humans. During the proliferative phase at the first half of the menstrual cycle, estrogen level is high. Following ovulation, the second half of the menstrual cycle is dominated by progesterone. In response to these hormones, the endometrium undergoes morphological and physiological changes. Progesterone transforms the endometrium and creates an uterine milieu ready for embryo attachment (2,21-23). Molecular and cellular mechanisms by which these hormones coordinate the development of embryo and uterus are poorly understood.

1.2.2 Decidualization

Implantation of the embryo into the uterine wall involves a complex and reciprocal relationship between the mother and the fetus (20,21). This maternal-fetal dialogue involves an intimate interaction between the specialized trophectodermal cells of the embryo and the receptive uterine lining of the mother. In mice, the steroid hormones E and P orchestrate the changes in the uterine epithelium that make it competent to attach to the blastocyst and initiate the process of implantation on day 4 of pregnancy (24,25).

In preparation for implantation, the human endometrium undergoes dramatic cyclic cellular and molecular developments in response to steroid hormones (2,21-23). A marked rise in the level of P along with a moderate increase in the level of E occurs during the post-ovulatory or luteal

phase of the cycle. These hormones transform the endometrium and make it receptive for embryo attachment (2,21-23). The underlying molecular and cellular mechanisms by which these hormones coordinate the development of embryo and uterus are poorly understood.

1.2.3 Angiogenesis

Angiogenesis, a characteristic event during implantation and decidualization, is critical for the growth and development of embryo. The process involves formation of new blood vessels from pre-existing vasculature in the uterus. Several studies have indicated that E and P play an important role in this process (26-28). Vascular endothelial growth factor (VEGF) (29,30) is recognized as a key regulatory growth factor for angiogenesis (31). Targeted deletion of the gene encoding *Vegf* results in embryonic death due to abnormal blood vessel formation (32,33). Certain members of the angiopoietin family including angiopoietin 1 and 2 are expressed in the endometrium and are known to modulate angiogenesis by promoting vascular maturation and remodeling (34,35). While it has been reported that E and P regulate the expression of these genes in the endometrium (36,37), the exact mechanism and signaling pathways by which these hormones regulate angiogenesis remain unclear.

1.2.4 Placentation

The placenta, a transient organ, physically connects the mammalian embryo to its mother. Establishment of this connection is absolutely critical for the growth of the embryo. The specialized cells of embryo including the trophoblast, endoderm, and extraembryonic mesoderm form early in development and attach the embryo to the uterus. During early placentation, the trophectoderm proliferates to form the ectoplacental cone, which later becomes the spongiotrphoblast layer. The outermost trophoblast cells of the ectoplacental cone differentiate and form the trophoblast giant cells, which form the interface with the maternal decidua.

Endoderm cells from the inner cell mass (ICM) form the Reichert's membrane. After gastrulation on day 7.5, the extraembryonic mesoderm forms the visceral yolk sac which differentiates to form hemangioblasts (7).

These cell lineages establish the three layers of the murine placenta. The zone closest to the chorionic plate is the labyrinth zone (38). Surrounding the labyrinth is the junctional zone of the murine placenta, which is composed of fetal spongiotrophoblasts and trophoblast glycogen cells. This is followed by a layer of trophoblast giant cells. The three layers of the murine placenta provide the means for communication between the mother and fetus. Although gene expression studies are being carried out to understand the functions of trophoblast lineages, the mechanism underlying the placental formation is not clear (5,39,40).

Embryonic day 10 is a critical juncture in the rodent placenta, when the chorioallantoic circulation becomes the primary support for the embryo. The placenta forms an essential maternal-fetal interface to exchange oxygen and nutrition to the growing fetus. During placentation, the fetal trophoblast cells invade into maternal decidua to reach spiral arteries and transform them into dilated vessels (41-46). As a result of trophoblast invasion, spiral arteries undergo dilation up to several times their original lumen diameter (47). Defects in invasion of fetal trophoblast cells into maternal decidua can result in various clinical problems such as, spontaneous abortion, preeclamsia, and intra uterine growth restriction (IUGR) (29,30,38,48-50). Due to the advancement of gene targeting technology, mouse models are becoming useful to study human pregnancy disorders (51,52)

1.2.5 Runx1- a member of Runx family of transcription factors

The Runx transcription factors derive their names from the founding members of the family, the drosophila runt genes. These genes play an important role in morphogenesis, sex determination

and eye formation in the fly (53). There are three family members including, Runx1, Runx2 and Runx3. RUNX genes encode the α-subunit, also termed as polyomavirus enhancer-binding protein 2 (PEBP2) α/core-binding factor (CBF) α, and combine with the β subunit (PEBP2β/CBFβ) to form the heterodimeric transcription factor (54,55). All three Runx proteins harbor a conserved 128 amino acid runt domain, which mediate hetero-dimerization with CBFβ and binding to DNA (56,57). The three RUNX genes are critical for the development of specific tissues. While Runx1 plays an important role in physiology of blood cells, Runx2 is critical for bone and Runx3 is critical for neurons of the dorsal root ganglia (58).

The Runx1 gene was first cloned in 1991 and targeted inactivation of this gene in mice led to complete blockade of definitive hematopoiesis and embryonic lethality between E12.5 and E13.5 (59,60). It has been reported that Runx1 is expressed in hematopoietic cells in the yolk sac and endothelial cells within the vitelline and umblical arteries of embryo at E10.5 (61). Runx1 also plays a supportive role in bone formation and can mediate oncogenic transformation to acute mylogenous leukemia (62-65).

1.2.6 Runx genes and reproductive tissues

Runx-dependent function in reproductive physiology has not been established so far. Runx1 and Runx2 are expressed during development in Müllerian ducts, which ultimately form the uterus, cervix, and the upper part of the vagina (66). In contrast, the expression of Runx1 and Runx2 is absent in Wolffian ducts, which form the epididymis and vas deferens. The functional role of Runx genes in the development and function of female reproductive tract remains unknown. In the adult, the ovarian expression of all three Runx genes have been reported previously (67-69). Runx1 and Runx2 have been shown to regulate key events during corpus luteum formation in mice and rat (70-72).

In pathophysiology, Runx1 expression has been associated with the development of endometrial invasive carcinoma. Interestingly, previous studies also indicated that ectopic expression of Runx1 leads to metastasis in a murine orthotopic model (73,74). While it has been reported previously that Runx1 expression is upregulated in endometriosis, no information is available about its uterine expression and its role during pregnancy and pregnancy related disorders.

My thesis is focused on the investigation of functional role of Runx1 at the maternal–fetal interface during early pregnancy.

CHAPTER 2
MATERIALS AND METHODS

2.1 Animals and Tissue Collection

Mice were maintained in the designated animal care facility at the College of Veterinary Medicine of the University of Illinois, Urbana-Champaign, according to the institutional guidelines for the care and use of laboratory animals. Control animals have two alleles flanked by lox P sites, termed *Runx1* "floxed" animals designated as $Runx1^{fl/fl}$. Experimental animals have two alleles flanked by lox P sites as well as one allele expressing cre-recombinase under the progesterone receptor promoter, termed *Runx1* "deleted" animals designated as $Runx1^{d/d}$.

To generate the conditional *Runx1*-null mice ($Runx1^{d/d}$), *Runx1*-floxed ($Runx1^{fl/fl}$) (75) mice were mated with PR-Cre knock-in mice (76). For breeding studies, cycling female $Runx1^{fl/fl}$ mice and $Runx1^{d/d}$ were housed with wild-type C57BL/6 male mice (Charles Rivers) for 6 months. The presence of a vaginal plug after mating was designated as day 1 of pregnancy. The number of litters and pups born were recorded at birth to assess the fertility status.

Mice were sacrificed by CO_2 overdose, and uterine, ovarian and other tissues were collected at various days of gestation. Tissues were either placed in fixative (10% Neutral Buffered Formalin-NBF, Fisher) or flash frozen in liquid nitrogen or subsequently stored at -80 ^{o}C.

Superovulation experiments were carried out using 7-8 week old female mice. The mice were injected intraperitoneally with 5 IU of Pregnant Mare Serum Gonadotropin (PMSG) and 48 hours later by 5 IU of human Chorionic Gonadotropin (hCG) and killed 16-18 h post hCG administration. Oocytes were flushed from the oviducts and counted. PMSG and hCG were purchased from Sigma Aldrich (St. Louis, MO).

Delayed Implantation was carried out by ovariectomizing mice on day 4 (morning) of pregnancy and injected subcutaneously with P in oil vehicle (2 mg) daily from days 5-7. To terminate delayed implantation and induce blastocyst attachment, the P-primed delayed implanting mice were given an injection of E in oil (50 ng) on the fourth day of the delay (day 8). Mice were euthanized at different time points after E injection and uteri were collected. Both progesterone and estrogen were purchased from Sigma Aldrich (St. Louis, MO).

Artificial decidualization reaction (77) was carried out as described previously (78). Mice of 7-8 weeks of age were ovariectomized and rested for two weeks. Mice were primed with three daily subcutaneous injections of 100 ng of 17α - estradiol in 0.1 ml cottonseed oil. Mice were given a brief rest without injections for two days and then received three daily injections of 2 mg P plus 6.7 ng of 17β - estradiol in 0.1 ml cottonseed oil. Six hours after the third injection, animals were anaesthetized and one horn of the uterus was stimulated by injecting 20 ul of cottonseed oil into the uterine horn. Daily injections of progesterone and estrogen were continued until the collection point for the uteri. The uteri were then extracted, weighted, and processed for immunohistochemical analysis.

Serum samples were collected on days 8, 10 and 12 of pregnancy after animals were euthenized by CO_2 overdose. Serum progesterone and estrogen concentrations were measured by radioimmunoassay (RIA) at the Ligand Core Facility of University of Virginia at Charlottesville. The values are expressed as mean +/- SEM.

2.2 Histology

Uterine and ovarian tissues collected on various days of gestation were fixed in neutral buffered formalin, processed and embedded in paraffin blocks. Sections (4μm) were utilized for

Hematoxylin and Eosin staining (H&E) and histological analysis. Image J software was used for morphometric measurement of decidual thickness.

2.3 Immunohistochemistry/Immunofluorescence

Uterine tissues were processed and subjected to immunohistochemistry as described previously (79). Paraffin-embedded tissues were sectioned at 4 μm and mounted on microscopic slides. Sections were deparaffinized in xylene, rehydrated through a series of ethanol washes, and finally rinsed in water. Antigen retrieval was performed by immersing the slides in 0.1M citrate buffer solution at pH 6.0, and by heating in the microwave for 25 min. The slides were allowed to cool and endogenous peroxidase activity was blocked by incubating sections in 0.3% hydrogen peroxide in methanol for 15 min at room temperature. After washing with PBS for 15 min, the slides were incubated in a blocking solution for 1 h before incubating them in primary antibody overnight at 4°C with antibodies specific for RUNX1(SC-28679), Progesterone Receptor (PGR-A0098, DAKO), CD31(BD Pharmingen 557355), Ki67(BD 550609), Prolactin Related Protein (PRP, -AB1293, Chemicon), Prolactin Like Protein –B (PLP-B, AB 1291, Chemicon), angiopoietin2 (ANG2, SC-7017), vascular endothelial growth factor –A (VEGF-A, SC-152), Cytokeratin8 (hybridoma bank, Troma 1), α-smooth muscle actin (α-SMA, ab-5694), platelet endothelial cell adhesion molecule (PECAM, SC-56), forkhead box protein O1 (FOXO1, Epitomics 1874-1) and Connexin 43 (Invitrogen 35-5000). Immunoflouerscence was carried out using Alexa fluor 488 or cy3 conjugated secondary antibodies from Jackson immunology and counter stained with DAPI. Immunofluorescence for all the proteins stained was repeated in uterine sections collected from 5 -8 animals.

2.4 Western blot analysis

Whole cell extracts were prepared from mouse uterine decidual cells isolated from day 8 pregnant uteri as described previously (80). Western blot analysis was performed following the protocol described previously (81). Briefly, cells were washed with ice-cold balanced solution

and lysed with the radioimmuneprecipitation assay buffer (0.1% SDS, 0.5% sodium deoxycholate, 1% Nonidet P-40 in PBS) containing protease inhibitor mixture, phenylmethylsulfonyl fluoride (PMSF, 0.1 mg/ml), and phosphatase inhibitor (1:1000; Sigma-Aldrich). The cells were passed through a 25-gauge syringe and centrifuged at 12,000 rpm for 10 min to remove the cell debris. of The protein (20–50 μg) extract was analyzed by SDS-PAGE and transferred to polyvinylidene fluoride membrane (Amersham Biosciences). The membrane was then blocked with 5% BSA in Tris-buffered saline with 0.1% tween 20 for 1 h at room temperature, followed by incubation with a primary antibody against Runx1, or calnexin. The blot was then incubated with the corresponding HRP-conjugate secondary antibody for 1hr at room temperature. Chemilumescence was utilized to detect HRP.

2.5 Alkaline Phosphatase Activity

Frozen tissue sections were used to detect alkaline phosphatase activity. Frozen tissue sections were thawed at room temperature for 10 minutes and fixed onto slides by incubating in Neutral Buffered Formalin (NBF) for 5 minutes. Following fixation, slides were washed in water and incubated in dark at 37 ^{o}C for 30 minutes in 2mM a-naphthyl phosphate (Sigma Aldrich) and 4mM Fast Violet (Sigma Aldrich) in 0.1 M Tris HCL, pH 8.7. Sections were again washed in water to remove excess reagents and then cover slipped.

2.6 Quantitative real time PCR analysis (QPCR)

Uterine tissue was homogenized and total RNA was extracted by using TRIZOL reagent, according to the manufacturer's protocol. cDNA was prepared by standard protocols. cDNA was amplified by quantitative PCR using gene-specific primers and SYBR Green probes (Applied Biosystems, Warringtom, UK). The expression level of *Rplpo* (36B4), a ribosomal phosphoprotein was used as internal control. For each treatment, the mean Ct and standard

deviation were calculated from individual Ct values obtained from three replicates of a sample. The normalized Ct in each sample was calculated as mean Ct of target gene subtracted by the mean Ct of internal control gene. After normalization, ΔΔCt was then calculated as the difference between the Ct values of the control and treatment sample. The fold change of gene expression in each sample relative to a control was computed as $2^{-\Delta\Delta Ct}$ (82). The mean fold induction and standard errors were calculated from three or more independent experiments.

2.7 TUNEL & Dolichos Biflorus Agglutinin (DBA) staining

TUNEL staining was carried out following manufacture's protocol (TUNEL based apoptosis detection assay, R&D systems, catalog # 4812-30-K). Uterine sections were deparaffinized by washing in xylene twice for 5 minutes each. Following this, slides were rehydrated and incubated with 1ug/ml proteinase K for 15 min at room temperature. After washing in PBS, sections were incubated with TUNEL reaction mixture for 60 min in a humid chamber at 37 ^{o}C. The slides were washed and incubated with FITC-conjugate for 30min at 37 ^{o}C. The slides were counterstained with DAPI following washings in PBS and cover slipped.

Day 10 – day 12 paraffin sections were deparaffinized using xylene and rehydrated by washing them through a series of alcohol solutions and a final wash in water. Slides were then incubated in 1% BSA for 30 minutes at room temperature. Sections were then incubated with DBA solution in BSA (vector labs, catalogue # B-1035) at 37 ºC for 2hrs. After washing, the slides were incubated with AEC for 25 min at room temperatures. Slides were cover slipped after washing the slides twice in PBS.

2.8 Statistical Analysis

Statistical analysis was performed by *t*-test or ANOVA. The values were expressed as mean ± SEM and considered significant if $p < 0.05$.

2.9 Quantitation using ImageJ

Java based image analysis software ImageJ (http://rsb.info.nih.gov/nih-image/), was utilized for the quantification of immunofluorescence of different proteins as described earlier (83,84). Thickness of decidual sections which were previously stained with hematoxylin and eosin were also measured using this software. Stained uterine sections from different samples (n=8) were used for quantitation.

CHAPTER 3

RESULTS

3.1 Estrogen induces *Runx1* expression in mouse uterus during early pregnancy

To understand the molecular basis of steroid hormonal regulation of implantation, it is critical to identify the steroid-regulated gene networks that underlie this process. In this study, we used a well-established delayed-implantation mouse model in which embryo attachment to the uterus depends on the administration of estrogen to progesterone-primed ovariectomized pregnant uteri. Using mouse oligonucleotide microarrays, we compared mRNA profiles of uteri of pregnant mice treated with progesterone alone or progesterone plus an implantation-initiating dose of estrogen (15,85). Our studies identified several mRNAs that were up- or down-regulated in the uteri of mice undergoing delayed implantation after 24 h of estrogen administration. One of the mRNAs whose level was robustly enhanced after estrogen treatment encoded the transcription factor, Runx1. The Runx1 protein expression during delayed implantation was investigated by immunohistochemistry (Fig. 1). The expression of Runx1 was not detectable in the stromal cells of uterine sections of progesterone-treated delayed animals before estrogen administration (Fig. 1, panel A). The level of Runx1 protein increased dramatically in the stromal cells underlying the implanted embryo in response to estrogen treatment (Fig. 1, panel B).

We further confirmed the estrogen regulation of Runx1 in non-pregnant ovariectomized mice treated with estrogen by immunohistochemistry. As shown in Fig. 2, a marked induction in Runx1 expression was observed in uterine stromal cells in response to estrogen treatment (panel B), whereas weak Runx1 expression was seen in oil-treated control uteri (panel A).

3.2 Spatio-temporal expression of *Runx1* during early pregnancy

We next examined the spatio-temporal expression of Runx1 in pregnant mouse uteri using QPCR and immunohistochemistry. While *Runx1* mRNA levels were low on day 4, a marked increase in Runx1 expression was observed on day 5 of pregnancy. A significant level of Runx1 expression continued untill day 10 of gestation (Fig. 4a). Consistent with the RNA profile (Fig. 3), we detected nuclear expression of Runx1 in stromal cells at the implantation site on day 5 of pregnancy (Fig. 4b). As pregnancy progressed to day 8, the expression of Runx1 continued in the decidualizing stromal cells (Fig. 4c-e). The expression of Runx1 then declined on day 10 of gestation (Fig. 4f). These results showed that Runx1 is localized in differentiating stromal cells and suggest a possible role of this transcription factor during decidualization process.

3.3 Uterine ablation of *Runx1* leads to severe sub fertility

Global deletion of *Runx1* gene is embryonic lethal, necessitating the development of conditional deletion of this gene to study its functions during implantation (60,86). We employed the Cre-LoxP strategy to create conditional knockout of *Runx1* in the uteri of adult mice. Transgenic mice expressing Cre under the control of the progesterone receptor (PR) promoter were previously used to ablate "floxed" genes selectively in cells expressing PR, including uterine cells (80,87-89). We, therefore, crossed the PR-Cre mice with mice harboring the "floxed" *Runx1* gene to create Runx1$^{d/d}$ mice. We confirmed the deletion of *Runx1* in the uteri of these mutant mice by QPCR, immunohistochemistry, and western blot analysis. As shown in Fig. 5, neither *Runx1* mRNA (panel A) nor Runx1 protein (panels B and C) was detected in uteri of *Runx1*$^{d/d}$ mice on day 8 of pregnancy, confirming successful abrogation of the *Runx1* gene in uteri of *Runx1*$^{d/d}$ mice.

We next assessed the impact of Runx1 ablation in female fertility by carrying out a six-month breeding study. As shown in Table 1, an average of 1.9 pups per litter were born to *Runx1*$^{d/d}$

mice, while an average of 7.0 pups per litter were born to *Runx1*$^{fl/fl}$ mice. These results indicated a severe fertility defect in Runx1-null females (Table 1).

3.4 Ovarian function is unaffected in *Runx1*$^{d/d}$ female mice

To investigate the cause of subfertility in *Runx1*$^{d/d}$ females, we examined their ovarian function by inducing superovulation. Prepubertal *Runx1*$^{fl/fl}$ and *Runx1*$^{d/d}$ mice were treated with a regimen of gonadotropin hormones as described in Materials and Methods. We observed that, upon gonadotropin stimulation, the number of eggs produced by *Runx1*$^{d/d}$ was comparable to that produced by the *Runx1*$^{fl/fl}$ females (Table 2). Ovarian sections collected from *Runx1*$^{fl/fl}$ and *Runx1*$^{d/d}$ pregnant females on day 8 of pregnancy showed formation of corpora lutea (Fig. 6A, panels a & b). In further support of normal ovarian activity, the serum levels of progesterone and estrogen were comparable in *Runx1*$^{fl/fl}$ and *Runx1*$^{d/d}$ females on day 8 of pregnancy (Fig. 6B). Collectively, these results suggested that the subfertility of *Runx1*$^{d/d}$ females is not due to impairment in the hypothalamic-pituitary-ovarian axis or lack of fertilization, but is likely due to defective implantation or pregnancy failure following implantation.

3.5 Subfertility in *Runx1*$^{d/d}$ mice is due to a defect in uterine function

To further investigate the fertility defect, blastocysts were flushed from *Runx1*$^{fl/fl}$ and *Runx1*$^{d/d}$ uteri and counted. No differences in the number or in morphology was observed in the two genotypes (data not shown). Examination of pregnant uteri from *Runx1*$^{fl/fl}$ and *Runx1*$^{d/d}$ mice on days 6-7 of gestation showed normal implantation sites (Fig. 7A). Expressions of alkaline phosphatase (Fig. 7B), Bone morphogenetic protein 2 (*Bmp2*) and Core enhancer binding protein beta (*Cebp/β*) (Fig. 7C), markers of stromal differentiation (80,90), were also comparable in the uteri of *Runx1*$^{fl/fl}$ and *Runx1*$^{d/d}$ mice, demonstrating that the early phases of decidualization were not affected in *Runx1*$^{d/d}$ mice. However, we observed that a significant number of embryos failed

to grow after day 10 of gestation and began to show signs of resorption (Fig. 8A). Upon dissection and removal of outer serosa and myometrial layers, it was apparent that the *Runx1*$^{d/d}$ endometrial component exhibited distinct hemorrhage (Fig. 8c&d). We further dissected the implantation sites and observed that unlike *Runx1*$^{fl/fl}$ samples, which had distinct embryos, trophoblast layers and decidua (Fig. 8A-e), *Runx1*$^{d/d}$ samples showed signs of embryo resorption with a dense decidua (Fig. 8A-f). As pregnancy progressed to day 12, many resorbed embryos were noted in *Runx1*$^{d/d}$ uteri (Fig. 8B-h). Dissection of implantation sites from *Runx1*$^{fl/fl}$ uteri revealed normal and healthy embryos (Fig. 8B-i), whereas most of the embryos in *Runx1*$^{d/d}$ uteri were resorbed (Fig. 8B-j).

3.6 Histological analysis of mid pregnancy implantation sites

Histological analysis showed that decidua from day 10 and day 12 *Runx1*$^{fl/fl}$ mice were well vascularized (Fig. 9, A- a&c). With the progression of gestation, the decidua becomes thinner to accommodate the growing embryo, which was clearly evident in *Runx1*$^{fl/fl}$ mice (as shown by the arrow in Fig. 9A- a&c). In contrast, the deciduas from *Runx1*$^{d/d}$ uteri were dense and avascularized (Fig. 9A- b&d). No obvious decidual regression was observed in these mice with the progression of pregnancy. To further support this observation, we measured the decidual thickness by utilizing ImageJ software. Uterine sections from *Runx1*$^{fl/fl}$ and *Runx1*$^{d/d}$ mice on day 10 and day 12 of pregnancy were used for these analyses. Our study revealed that deciduas from *Runx1*$^{d/d}$ mice were twice as thick as the deciduas from control mice (Fig. 9B). Taken together, these results indicated that in the absence of uterine *Runx1*, the decidua fails to undergo regression during the progression of pregnancy.

3.7 Deletion of *Runx1* leads to persistent stromal cell proliferation in the uterus

To gain an insight into the underlying mechanism of non-regressed decidua in Runx1$^{d/d}$ mice, we monitored uterine proliferation. To specifically address the proliferation of uterine stromal cells, we performed co-localization of KI67, a marker of cell proliferation, and PR (91) in uterine sections on day 10 of pregnancy. As shown in Fig. 10a, an abnormally high numbers of PR positive decidual cells were observed in *Runx1*$^{d/d}$ uteri compared to *Runx1*$^{fl/fl}$ controls. Upon co-localization with KI67, we found that in contrast to *Runx1*$^{fl/fl}$ decidual cells, decidual cells in *Runx1*$^{d/d}$ uteri were highly proliferative (Fig. 10, compare c and d). Consistent with this observation, we noted a marked enhancement in the expression of cyclin D3 in *Runx1*$^{d/d}$ uterine sections compared to uterine sections from *Runx1*-intact mice (Fig. 11A). We also observed that the mRNA levels of Cdkn1b and c, inhibitors of cell cycle, were significantly lower in *Runx1*$^{d/d}$ uteri compared to *Runx1*$^{fl/fl}$ controls (Fig. 11B). Collectively, these results indicate that *Runx1* regulates cyclins and cyclin-dependent kinase inhibitors in uterine stromal cells and causes enhanced proliferation.

A recent report has shown that downregulation of a transcription factor, *Foxo1*, in human endometrial stromal cells promotes cellular proliferation by regulating *Cdkn1c* and cyclins (92). Impaired *Foxo1* expression has been associated with proliferative endometrial disorders such as endometriosis and endometrial cancer (93,94). When we monitored the expression of *Foxo1*, we noted with interest a marked down regulation of *Foxo1* in uterine sections of *Runx1*$^{d/d}$ compared to *Runx1*$^{fl/fl}$ uteri (Fig. 12 compare c & d). Conversely, TUNEL staining showed a decrease in the number of apoptotic decidual cells in *Runx1*$^{d/d}$ uterine sections compared to *Runx1*$^{fl/fl}$ controls (Fig. 13 compare c & d). The apparent lack of apoptotic cells in the abnormally dense decidua of *Runx1*$^{d/d}$ mice further confirms that uterine ablation of *Runx1* leads to extensive proliferation and a decline in apoptosis.

3.8 Impaired terminal differentiation of decidual cells in *Runx1*$^{d/d}$ uteri

Decidualization of stromal cells involves proliferation followed by differentiation. Since uteri from *Runx1*$^{d/d}$ mice show extensive proliferation, it was of interest to determine whether the decidual cells are able to undergo terminal differentiation. We, therefore, monitored the expression of well-known biomarkers of terminal differentiation such as *Prl8a2* (dPRP) and *Prl6a1* (PLP-B) (result not shown) (95-99). As shown in Fig. 14, the expression of *Prl8a2* (dPRP) was markedly downregulated in the decidual cell of *Runx1*$^{d/d}$ uteri compared to *Runx1*-intact control uteri.

The gap junction protein Connexin 43 or *Gja1* has been reported previously to be expressed in differentiating stromal cells during decidualization (88). We next investigated whether the expression of *Gja1* was altered in *Runx1*$^{d/d}$ decidua on day 9 of pregnancy by QPCR and immunohistochemistry. Our studies revealed that the expression of connexin 43 mRNA and protein was markedly down regulated in *Runx1*$^{d/d}$ uteri compared to *Runx1*$^{fl/fl}$ control (Fig. 15A & B). Collectively, these results indicate that uterine ablation of Runx1 impairs terminal differentiation of stromal cells.

3.9 *Runx1*$^{d/d}$ mice exhibit impaired angiogenesis during early pregnancy

Our previous studies indicated that a loss of gap junction communication mediated by connexin 43 between decidual cells impairs neovascularization during early pregnancy (88). Since the expression of connexin 43 is downregulated in *Runx1*$^{d/d}$ uteri, we next investigated the levels of angiogenic factors such as angiopoietin 2 and Vegf-A in *Runx1*$^{fl/fl}$ and *Runx1*$^{d/d}$ uteri on day 9 of gestation (Fig. 16). Our studies revealed a marked downregulation of angiopoietin 2 and Vegf-A mRNAs (Fig. 16 A and B) as well as angiopoietin 2 and Vegf-A proteins (Fig. 16C) in *Runx1*-null uteri.

Consistent with this observation, our studies revealed impaired angiogenesis as indicated by the expression of PECAM, a well-known endothelial biomarker (77,100,101), in *Runx1*$^{d/d}$ uteri (Fig. 17). While vascular network was well organized in *Runx1*$^{fl/fl}$ uteri, we noted disorganized vascular network with reduced PECAM staining in *Runx1*$^{d/d}$ (Fig. 17, compare a and b). Collectively, these results indicated that attenuation of stromal differentiation mediated by the loss of *Runx1* impairs angiogenesis during early pregnancy.

3.10 Abnormal maternal vascular remodeling and impaired trophoblast invasion in *Runx1*$^{d/d}$ decidua during mid-pregnancy

Maternal spiral artery modification manifested by the loss of α-smooth muscle actin (α-SMA) in spiral artery, is a characteristic feature during mid-pregnancy (45,102,103). This modification is achieved when the invading trophoblast cells reach the spiral artery. Since *Runx1*$^{d/d}$ uteri exhibit dense decidua, it raises an interesting possibility that trophoblast cells are unable to migrate through dense decidua to reach and transform the maternal spiral arteries. To investigate this possibility, we monitored the expression of α-SMA in uterine spiral arteries of *Runx1*$^{fl/fl}$ and *Runx1*$^{d/d}$ mice on day 12 of pregnancy (Fig. 18). SMA staining on spiral arteries at four specific regions in the maternal decidua was closely investigated. Staining in radial artery (Fig. 18A-a and 18B-e), spiral artery in myometrium (Fig. 18A-b and 18B-f), distal region of the endometrium (at the edge of decidua close to myometrium) (Fig. 18A-c and 18B-g) and proximal region (closer to labyrinth) (Fig. 18A-d and 18B-h) were observed. In *Runx1*$^{fl/fl}$ uteri, as expected, the radial artery showed intense α-SMA staining (Fig. 18A-a). The staining was less intense in the myometrial spiral artery (Fig. 18A-b), very weak in the distal artery (fig 18A-c) and was completely absent in the proximal artery (Fig. 18A-d). On the other hand, *Runx1*$^{d/d}$ uteri exhibited distinct α-SMA staining in the spiral arteries at all four regions (Fig. 18B-e, f, g and h).

Persistent expression of α-SMA in *Runx1*$^{d/d}$ distal and proximal endometrial spiral arteries clearly suggests that vascular remodeling is affected by the loss of *Runx1*.

We next investigated the invasion of trophoblasts in *Runx1*$^{fl/fl}$ and *Runx1*$^{d/d}$ decidua by monitoring the expression of cytokeratin 8 (Troma 1), a marker of trophoblast cells (Fig. 19). Cytokeratin 8 positive migrating trophoblasts were clearly observed, in maternal decidua of *Runx1*$^{fl/fl}$ uteri. However, deciduas of *Runx1*$^{d/d}$ uteri were totally devoid of cytokeratin 8 positive invading trophoblastic cells. Since endovascular invasion of trophoblast cells into spiral arteries leads to modification and the loss of the smooth muscle layer (104), we next co-localized cytokeratin 8 and α-SMA in uterine sections of *Runx1*$^{fl/fl}$ and *Runx1*$^{d/d}$ uteri on day 12 of pregnancy (Fig. 20). Our results showed that in the *Runx1*$^{fl/fl}$ uterine sections, as expected, spiral arteries proximal to the placenta were positive for cytokeratin 8 with weak α-SMA staining (Fig. 20b). In contrast, the proximal spiral arteries in *Runx1*$^{d/d}$ uterine sections exhibited strong α-SMA staining and minimal cytokeratin 8 staining (Fig. 20d). To rule out the possibility that there might be a delay in trophoblast migration, double immunofluorescence was carried out also in pregnant uteri on day 15 of pregnancy (Fig. 21). Our studies revealed extensive endovascular and interstitial trophoblast migration all the way up to the myometrium in *Runx1*$^{fl/fl}$ decidua (Fig. 21a). However, pregnant *Runx1*$^{d/d}$ uteri exhibited impaired trophoblast migration (Fig. 21c) and spiral artery modification (Fig. 21d) even in day 15. These results indicate that trophoblast migration is inhibited in *Runx1*$^{d/d}$ mice up to day 15 of pregnancy, which in turn contributes to insufficient spiral arterial modification. This led to restricted growth of fetus in *Runx1* $^{d/d}$ uteri. Interestingly, these are characteristic features of shallow placentation (30).

Previous studies have suggested that uterine natural killer cells or uNK (78), which are abundantly present in the decidua, mediate initial stages of remodeling in the spiral artery

(102,105-108). We, therefore, investigated whether poor spiral artery remodeling is due to any change in uNK cell population in *Runx1*$^{d/d}$ decidua by monitoring the expression of *Dolichos biflorus agglutinin* (DBA) lectin, which marks the uNK cells (Fig. 22). We observed that DBA positive uNK cells in *Runx1*$^{d/d}$ decidua (Fig. 22c) were at least 25-30% more in comparison to control *Runx1*$^{fl/fl}$ decidua (Fig. 22a). This was due to the persistent proliferation of uNK cells in *Runx1*$^{d/d}$ decidua as indicated by co-localization of DBA and Ki67 (Fig. 22, compare b & d). Taken together, these results indicated that deletion of *Runx1* in stromal cells perturbed the differentiation program and altered the decidual environment. This in turn affected maternal-fetal interactions causing insufficient blood and nutrient flow to the growing fetus, leading to fetal growth restrictions and fetal death.

CHAPTER 4
DISCUSSION

Successful implantation in rodents is dependent on the nidatory surge of estrogen on day 4 of pregnancy (2,3). While the implantation-inducing action of estrogen has been known for a long time, the factors that are functioning downstream of estrogen signaling to regulate implantation remain largely unknown. Gene expression profiling was useful in identifying *Runx1* as one of the mediators of estrogen action in uterus during delayed implantation. *Runx1* belongs to Runt family of transcription factors, which are known to play critical role during development. In this study we report for the first time the expression of *Runx1* in uterine stromal cells during early pregnancy. We further show that the expression of *Runx1* coincides with the decidual phase of pregnancy. While it is clear that estrogen induces *Runx1* expression in the uterus, the exact mechanism by which this hormone promotes *Runx1* expression remains unknown.

Analysis of *Runx1*-deficient uteri indicated persistent proliferation of endometrial stromal cells during decidualization. While this did not affect the early stromal differentiation program as indicated by the expression of alkaline phosphatase, *Bmp2* and *C/ebpβ*, we observed a marked defect in terminal differentiation of endometrial stromal cells due to ablation of Runx1. This was confirmed by the altered expression of a panel of biomarkers of stromal differentiation including *Gja1*, *Prl8a2* and *Prl6a1* in Runx1-null uteri. It is known that terminal differentiation of endometrial stromal cells is critical for establishment of pregnancy by entering the apoptotic pathway. This regression of decidua is pivotal for accommodation of growing fetus. Impaired terminal differentiation of stromal cells and lack of apoptosis in *Runx1* deficient uteri led to dense decidua, which failed to undergo regression and support maintenance of pregnancy.

Silencing *Foxo1* in differentiating human endometrial stromal cells promotes proliferation (92) which is similar to the observation in *Runx1* mice. Interestingly a conditional mutant of *Foxo1* exhibits similar phenotype as *Runx1* ablated mice (Dr. DeMayo's lab, unpublished observation). This raises the interesting possibility that *Foxo1* might be a downstream target of *Runx1* in the uterus during early pregnancy. Further detailed studies are needed to conclusively prove this hypothesis.

Tissue remodeling plays a critical role during decidualization and placentation, which involves changes in extra cellular matrix (ECM). This process is mediated by a variety of factors including transcription factors, proteases, cell surface receptors, and growth factors (102). Any modification in ECM turnover or degradation could affect decidual regression and reorganization. It is possible that impairment in terminal differentiation program in *Runx1*$^{d/d}$ decidua may also affect the expression of ECM molecules such as MMPs and TIMPs, causing a failure in decidual regression and dysregulated tissue remodeling (109,110). We speculate that the loss of *Runx1* from stromal cells adversely affects the communication between stromal cells and release of factors essential to degrade extra cellular scaffolding affecting tissue and vascular remodeling. In totality, these defects result in shallow implantation, poor fetal-maternal circulation, inadequate embryonic development, and ultimately fetal death.

It has been shown previously, that stromal cell differentiation and angiogenesis are linked events during decidualization (88). Angiogenic factors are secreted by the differentiated decidual cells, which are involved in promoting neovascularization at the mesometrial decidua. Uterine deletion of *Runx1* caused attenuation of connexin 43 expression, which in turn led to reduced expression of angiogenic factors such as angiopoietin2 and Vegf-A causing defective angiogenesis in decidua of *Runx1*$^{d/d}$ mice.

In summary, our study demonstrates that *Runx1* expressed in the stromal cells acts on several uterine cell types to regulate critical physiological processes, including stromal differentiation, decidual regression, trophoblast invasion, maternal vascular remodeling and immune modification (Fig. 23). We propose that this *Runx1*$^{d/d}$ mouse model will be an important model to study human pregnancy disorders such as spontaneous abortion, intra-uterine growth restriction and preeclampsia.

FIGURES AND TABLES

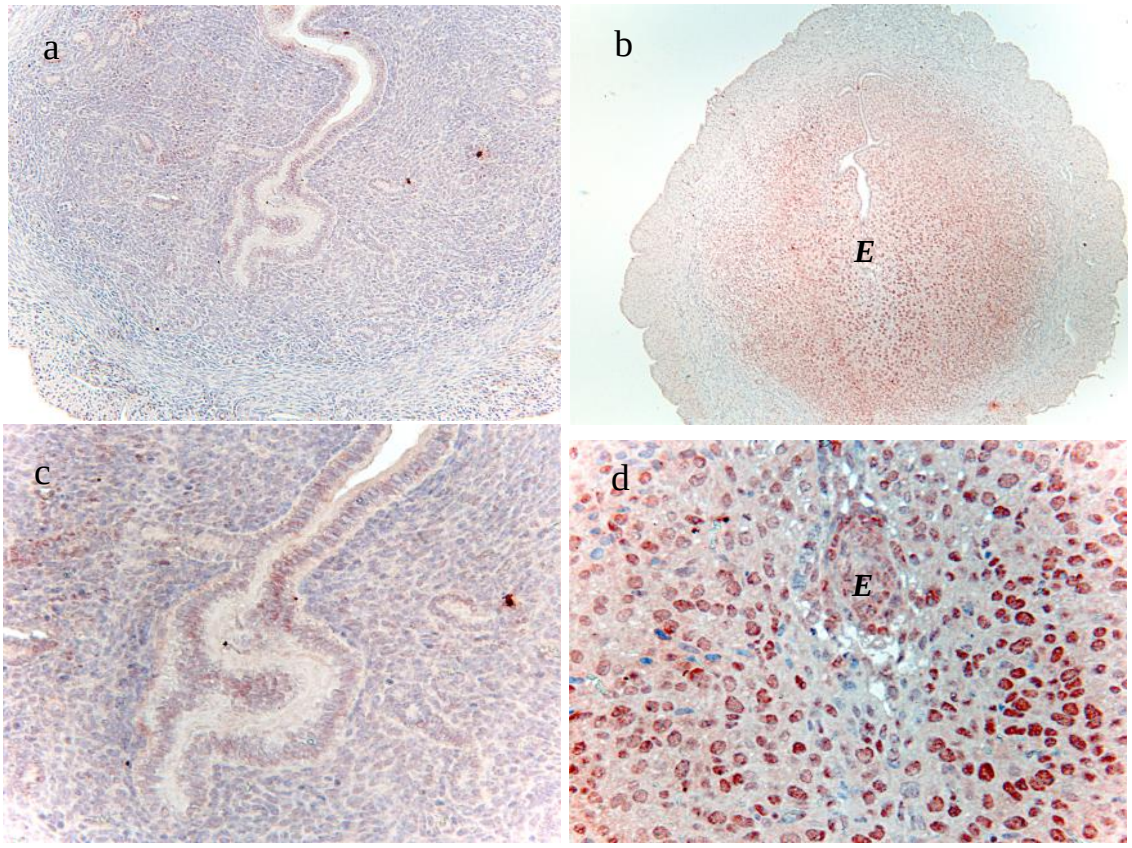

Fig. 1 Induction of Runx1in uterine stromal cells during delayed implantation.

The delayed implantation mouse model was used to analyze Runx1 protein expression. Uteri were subjected to a delayed embryo implantation protocol and collected at (b) 24 h following estrogen treatment and subjected to IHC using anti-Runx1 antibody. Figures a-b were taken at 4x magnification. Panel c and d represents 20x magnification of a & b. The 0-h sample (panel a) represents a pregnant uterus obtained from a mouse treated with progesterone alone for three days.
E: embryo

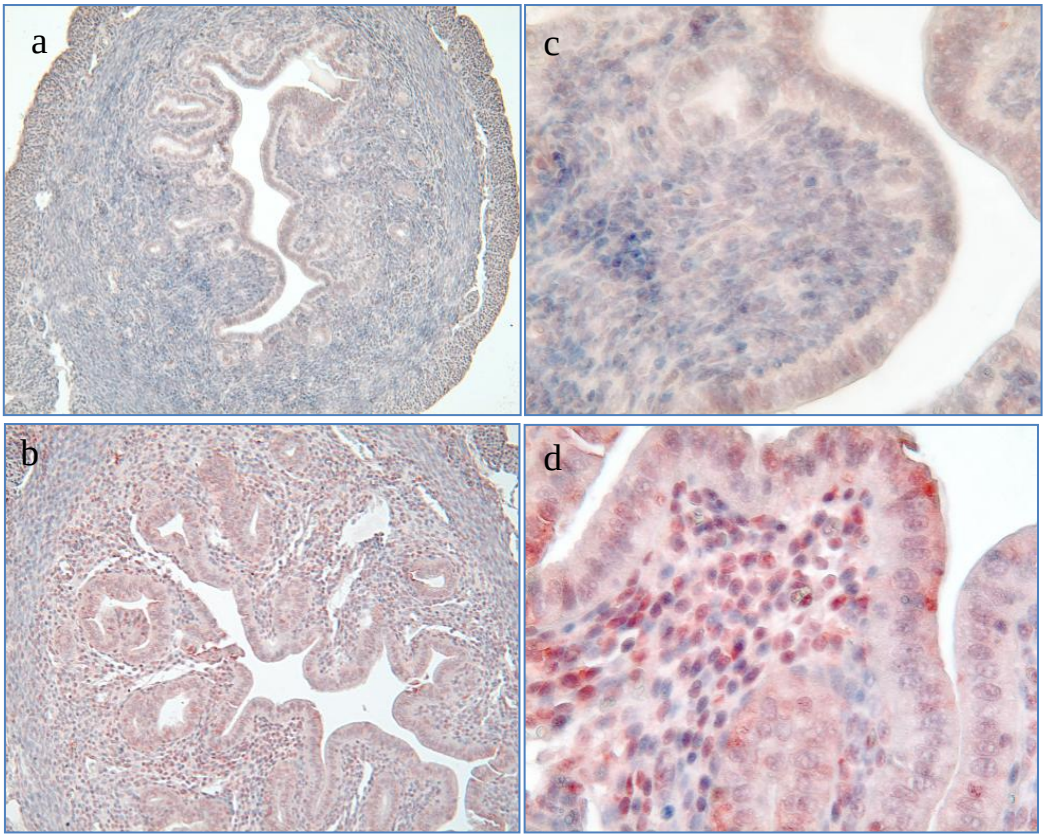

Fig. 2 Estrogen induces Runx1 in the uterus

Ovariectomized mice were treated with oil and estrogen and uterine samples were collected after 24h. Uterine sections were subjected to immunohistochemistry using anti-Runx1 antibody. Panels a & c are oil treated control samples and panels b& d are estrogen treated samples. Panels c & d are 20x magnification.

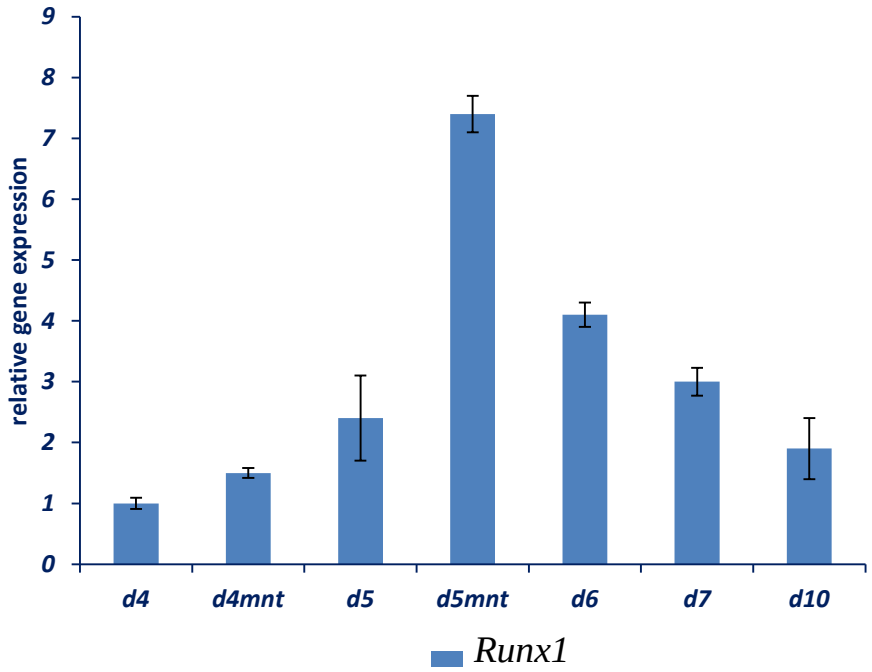

Fig. 3 mRNA profile of Runx1 expression during pregnancy

Real time PCR was carried out to study the expression profile of *Runx1* during pregnancy. The relative levels of gene expression at different days of pregnancy were determined by setting expression level on day 4 of pregnancy as 1.0 and *Rplpo*, encoding ribosomal protein level was used for normalization.n= five, p=< 0.05

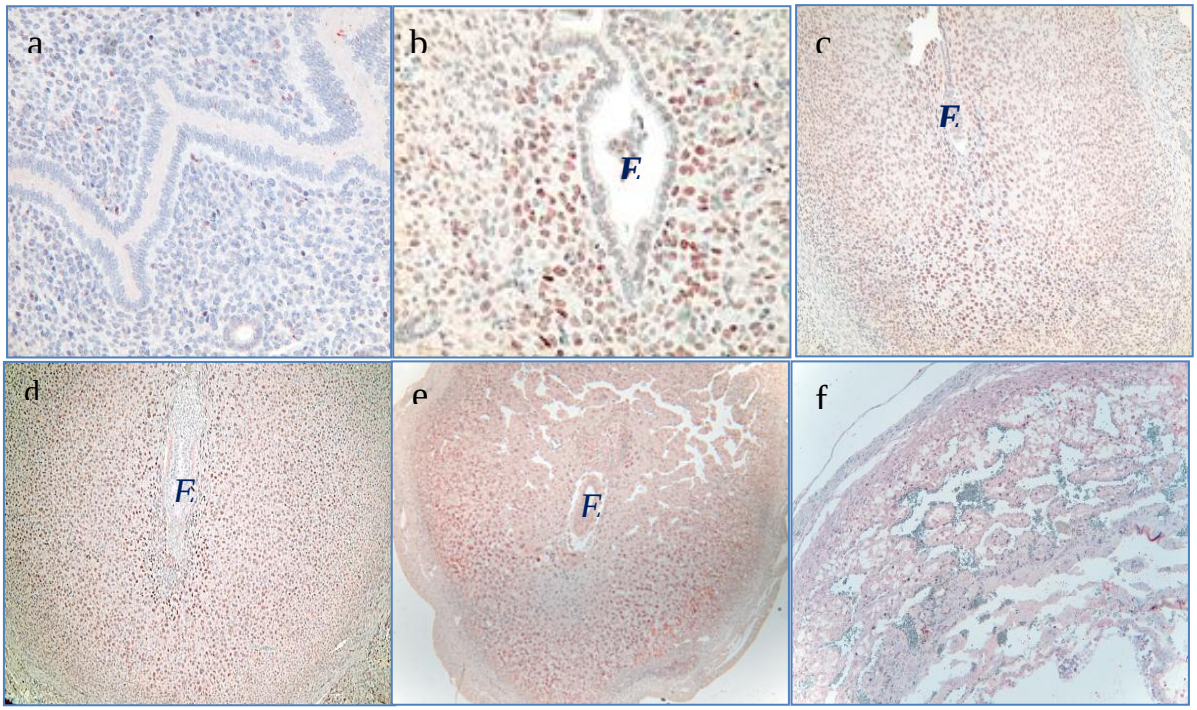

Fig. 4 Spatio-Temporal expression of Runx1 in mouse uteri during pregnancy

Uterine sections of day 4 - day 10 pregnant uteri (panels a-f) were subjected to immunohistochemistry analysis using anti-Runx1 antibody. E indicates embryo. Hematoxylin is used as counterstain.

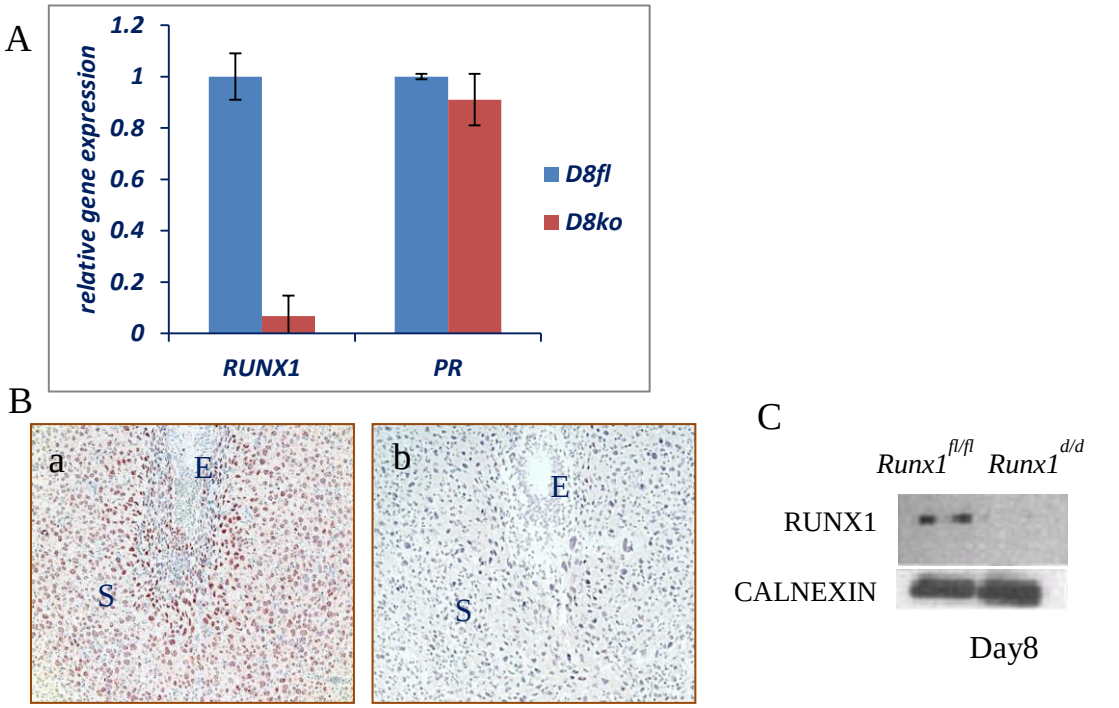

Fig. 5 Detection of RUNX1 in day 8 uteri of *Runx1*$^{fl/fl}$ and *Runx1*$^{d/d}$ mice.

Real time PCR of *Runx1* mRNA (A) was examined. mRNA level in Runx1$^{d/d}$ uteri were compared with that of *Runx1*$^{fl/fl}$ using *Rplpo*, encoding ribosomal protein level for normalization, *p < 0.01. Immunohistochemistry of Runx1protein (B) was carried out using anti-RUNX1 antibody in *Runx1*$^{fl/fl}$ (a) and *Runx1*$^{d/d}$ (b) uterine sections. Western blot analysis (C) of RUNX1 protein was analyzed in uterine decidual cell protein extract. Calnexin was used as loading control.

Table. 1 Ablation of *Runx1* impairs female fertility

Genotype	*No. of animals*	*No. of Litters born**	*No. of litters per animal (Mean ± SE)*	*No. of pups born*	*No. of pups per litter‡ (Mean ± SE)*
$Runx1^{f/f}$	*6*	*21*	*3.50± 0.56*	*147*	*7.0±0.47*
$Runx1^{d/d}$	*6*	*10*	*1.67± 0.56*	*19*	*1.9±0.28*

**Results of a six-month breeding experiment.* ‡ *p=0.0001*

Table. 2 Deletion of *Runx1* does not affect ovarian function

	# of oocyte/ ovary	*Mean ±SE **
$Runx1^{fl/fl}$	*127/10*	*12.7± 3.0*
$Runx1^{d/d}$	*103/10*	*10.3± 2.0*

*p =0.52

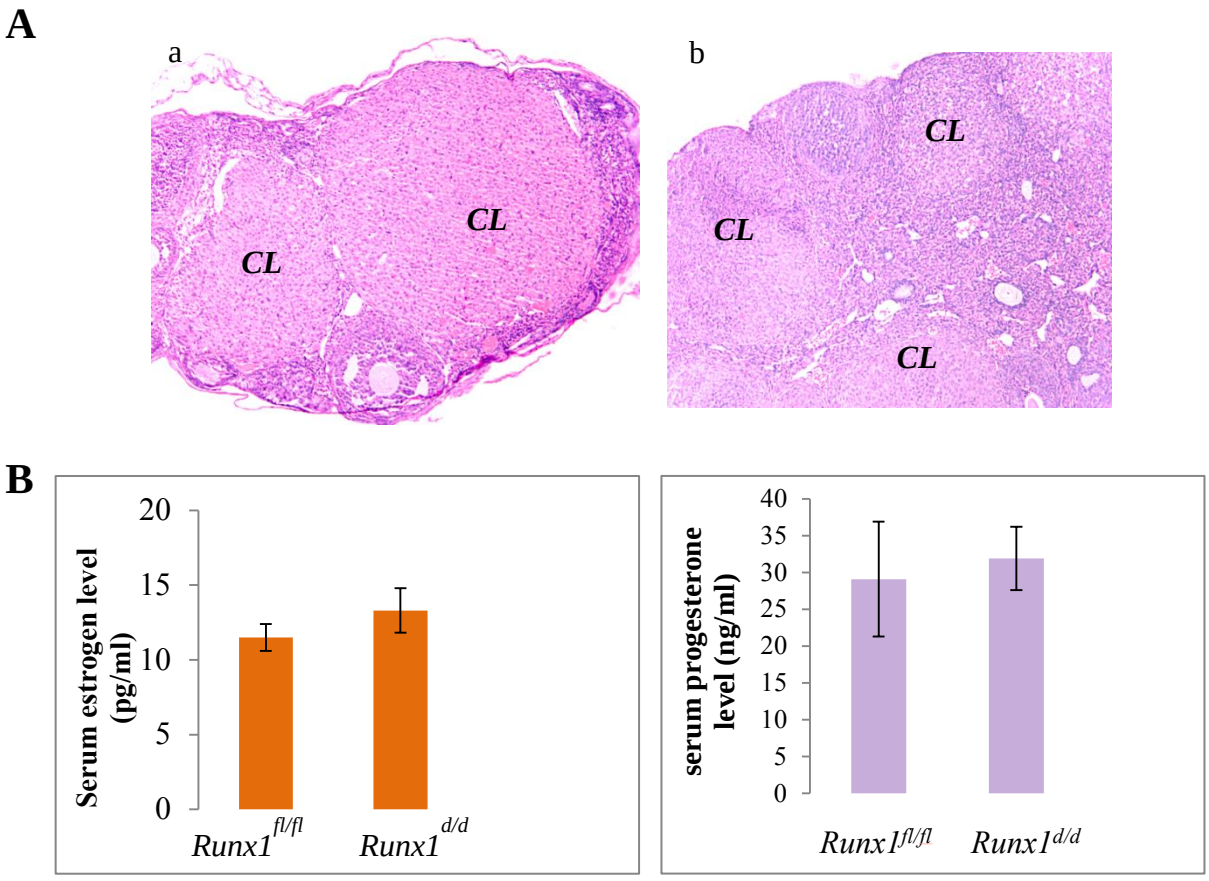

Fig. 6 Deletion of *Runx1* does not affect ovarian function

(A) H&E staining of day 8 pregnant uteri of (a) *Runx1*$^{fl/fl}$ *and (b) Runx1*$^{d/d}$ mice

(B) Serum hormonal levels of estrogen (p=0.078) and progesterone (p=0.27) in day 8 pregnant mice (n=8).

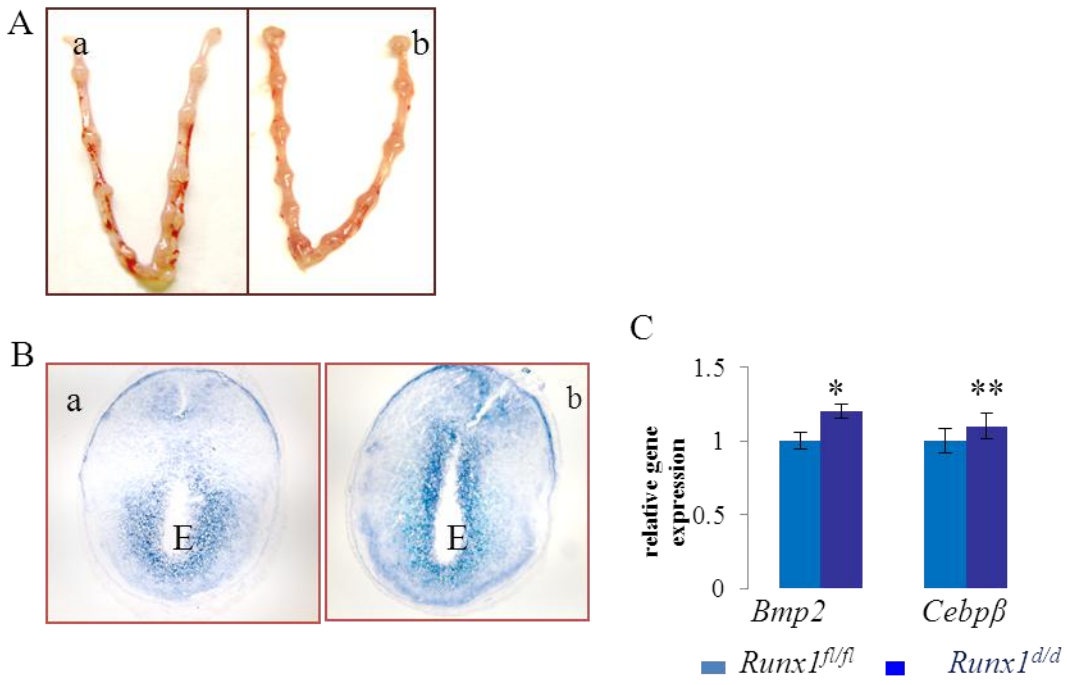

Fig. 7 Embryo attachment and initial phases of decidualization are unaffected in *Runx1*$^{d/d}$ mice

(A) Day6 pregnant uteri of *Runx1*$^{fl/fl}$ (a) and *Runx1*$^{d/d}$ (b) were collected.
(B) Alkaline phosphatase enzymatic activity was analyzed in frozen sections of *Runx1*$^{fl/fl}$ (a) and *Runx1*$^{d/d}$ (b) day7 pregnant uteri.
(C) mRNA levels of *Bmp2* and *Cebpb* were analyzed by real time QPCR. Level of *Rplp0* used as internal control for normalization.
*p=0.062 and **p = 0.09,
E: Embryo

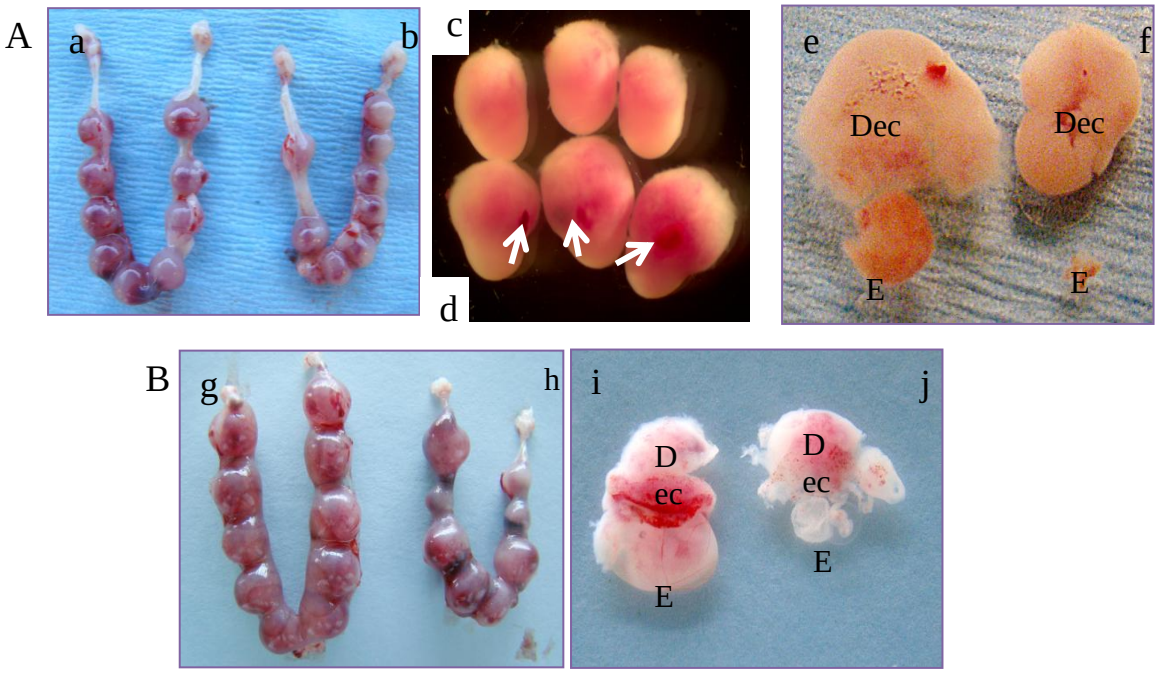

Fig. 8 Ablation of *Runx1* leads to embryo resorption during mid-pregnancy

Day10 and day12 pregnant uteri (A & B) were collected and analyzed. Implantation sites of day10 *Runx1*$^{fl/fl}$ (a,c & e) and *Runx1*$^{d/d}$ (b,d & f) were dissected. Hemorrhaging sites are indicated by arrows. Similarly day12 implantation sites of *Runx1*$^{fl/fl}$ (B-g &i) and *Runx1*$^{d/d}$ (B-h &j) were dissected. Normal and healthy embryos were observed in day10 and day12 implantation sites of *Runx1*$^{fl/fl}$ uteri (a & g), whereas resorbed embryos were seen in *Runx1*$^{d/d}$ uteri (b & h). Dec: decidua and E: embryo.

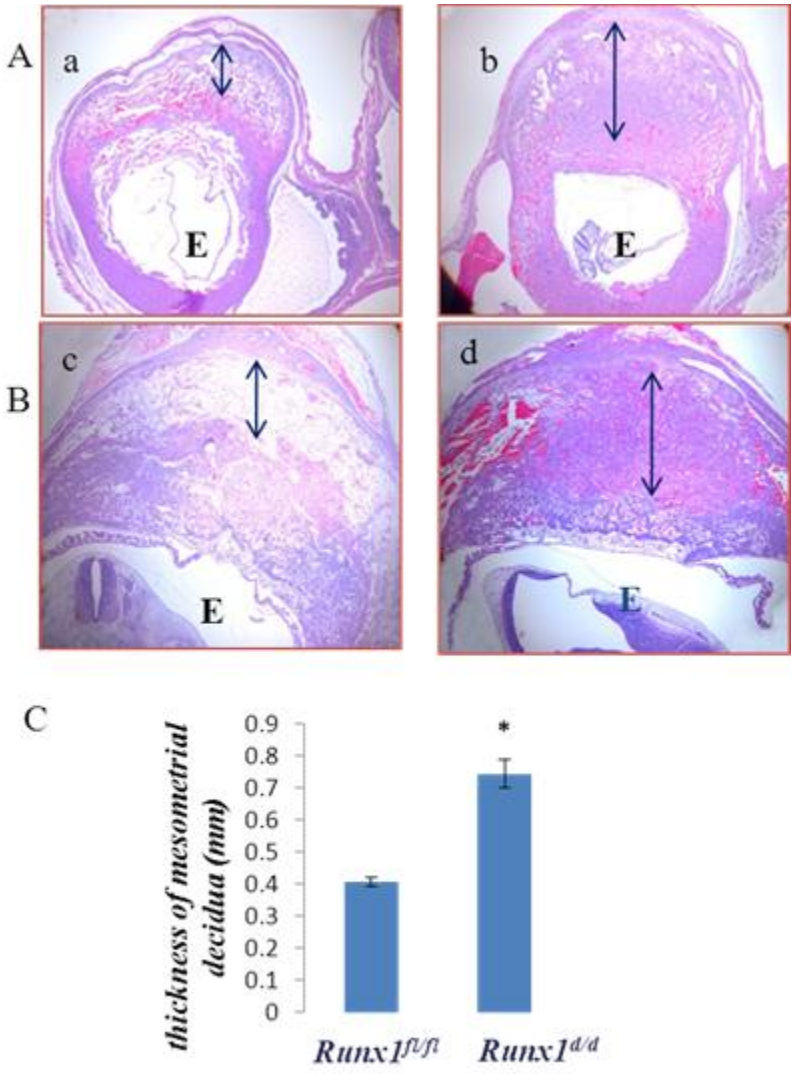

Fig. 9 Histology of H & E stained mid-pregnant implantation sites

Mid-pregnant day 10 A (a- *Runx1* $^{fl/fl}$ & b- *Runx1* $^{d/d}$) and day 12 B (c- *Runx1* $^{fl/fl}$ &d – *Runx1* $^{d/d}$) sections were stained with hematoxylin and eosin. Double arrow indicates decidua.
E indicates embryo.
C. Quantitation of day 10 decidual thickness using ImageJ software. N=8
*****$p < 0.0001$

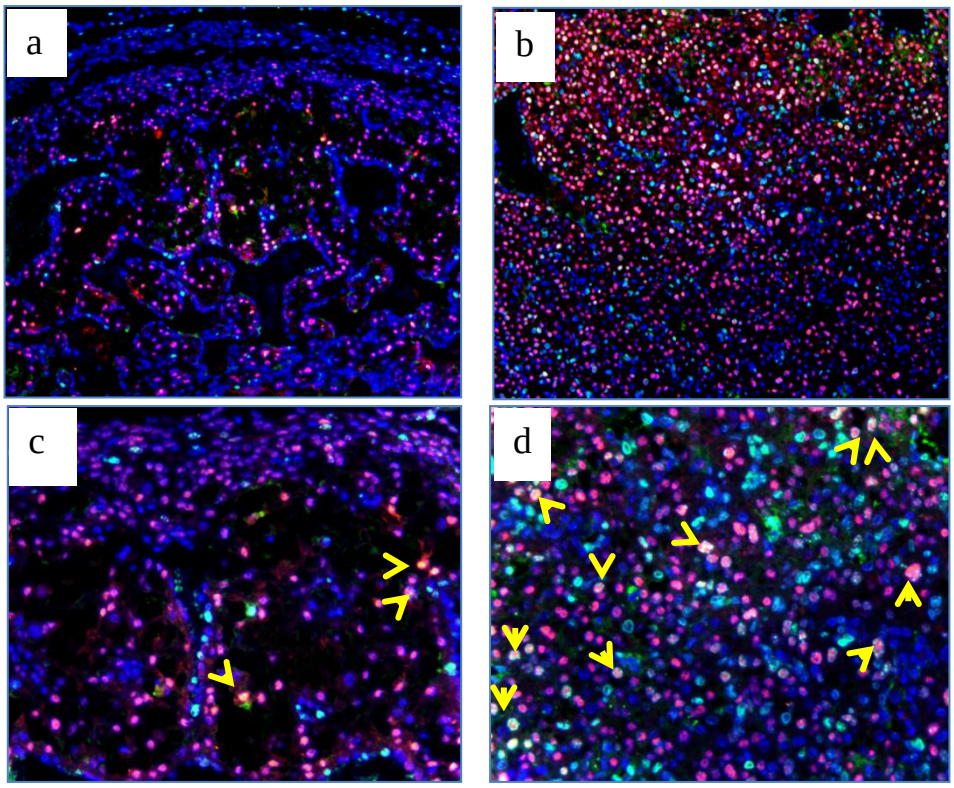

Fig. 10 Persistent proliferation of mesometrial decidual cells of *Runx1*$^{d/d}$ mice

Day10 uterine sections were colocalized using Ki67 (FITC) and PR (Cy3) antibodies. *Runx1*$^{fl/fl}$ (a&c) *Runx1*$^{d/d}$ (b & d), a & b are 10x, c & d are 20x magnification of day10 sections. Colocalized cells were indicated bv vellow arrowheads.

A

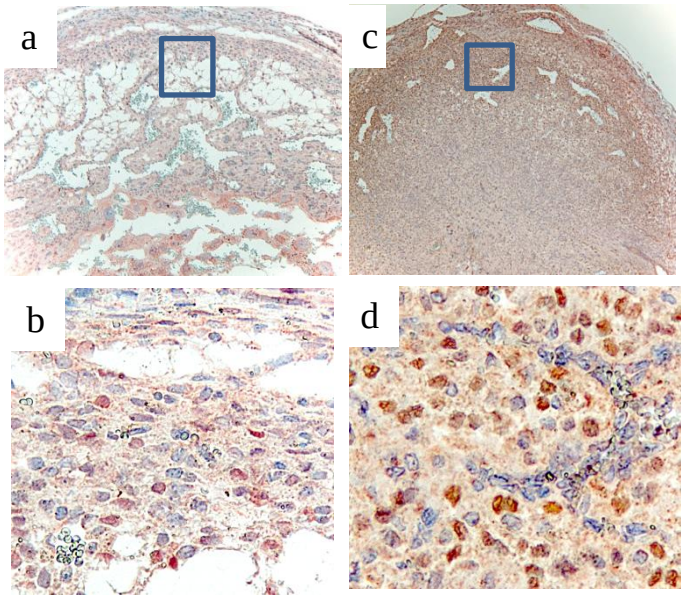

B

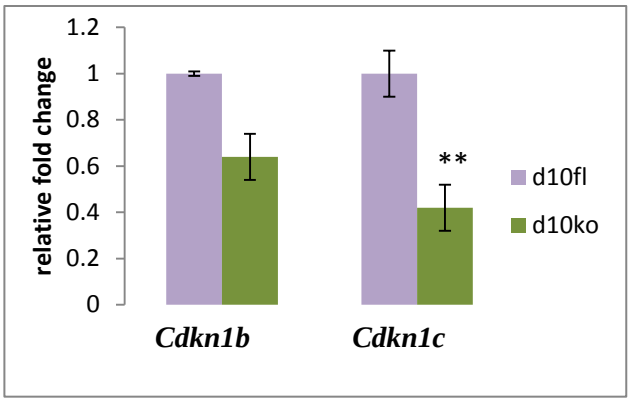

Fig. 11 Modified cell cycle molecules in *Runx1*$^{d/d}$ decidua

(A) Localization of CCND3 protein in d10 uterine sections of *Runx1*$^{fl/fl}$ (a & b) and *Runx1*$^{d/d}$ (c &d) were carried out. 40x magnification of boxed regions were shown in b & d.
(B) QPCR was utilized to measure mRNA levels of Cdkn1b and Cdkn1c. The level of *Rplp0* was used as internal control for normalization. *p < 0.01, **p <0.001

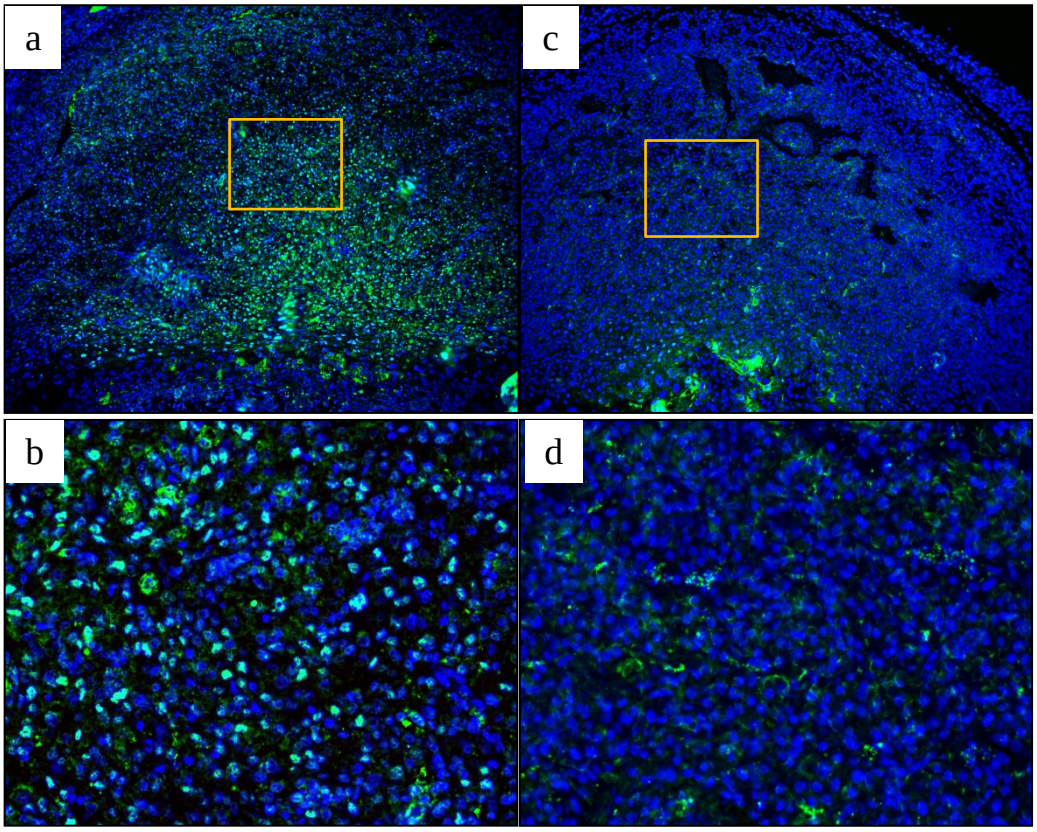

Fig. 12 Down regulation of *Foxo1* expression due to *Runx1* deletion

Localization of *Foxo1* protein in day10 uterine sections of *Runx1*$^{fl/fl}$ (a & b) and *Runx1*$^{d/d}$ mice (c &d).
20x magnification of boxed area of control and *Runx1*$^{d/d}$ sections are shown in b & d respectively

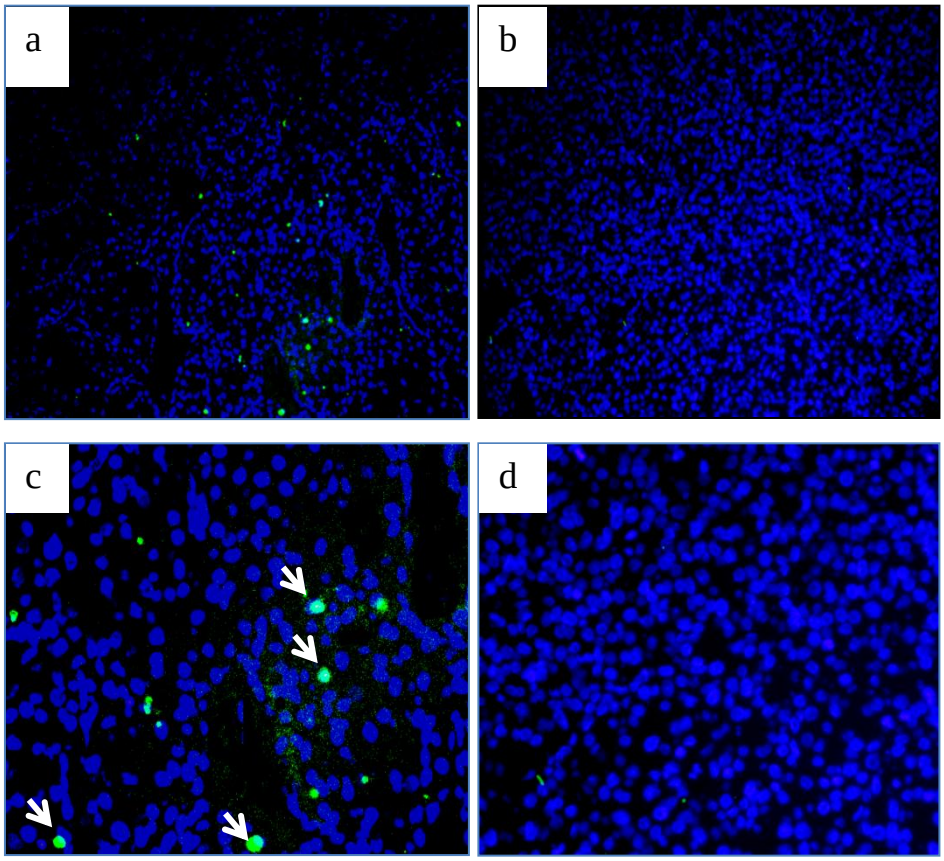

Fig. 13 Lack of apoptotic cells in day10 *Runx1*$^{d/d}$ *decidua.*

TUNEL staining was utilized to investigate apoptosis at day10 pregnancy of *Runx1*$^{fl/fl}$ (a & b) and *Runx1*$^{d/d}$ (b & d) uterine sections. Apoptotic cells are marked by arrows. a & b were 10x, c & d were 20x magnification.

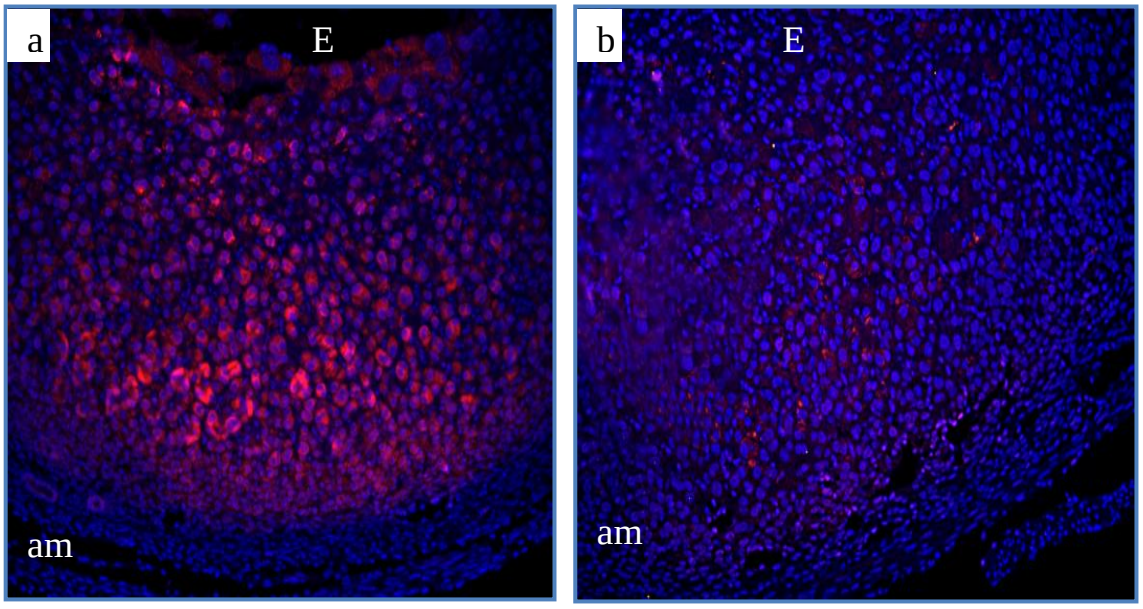

Fig. 14 Terminal differentiation is attenuated in *Runx1*$^{d/d}$ decidua

Localization of *Prl8a2* (dPRP) protein in day 9 uterine sections of *Runx1*$^{fl/fl}$ (a) and *Runx1*$^{d/d}$ (b).
E : embryo and am: anti mesometrial.

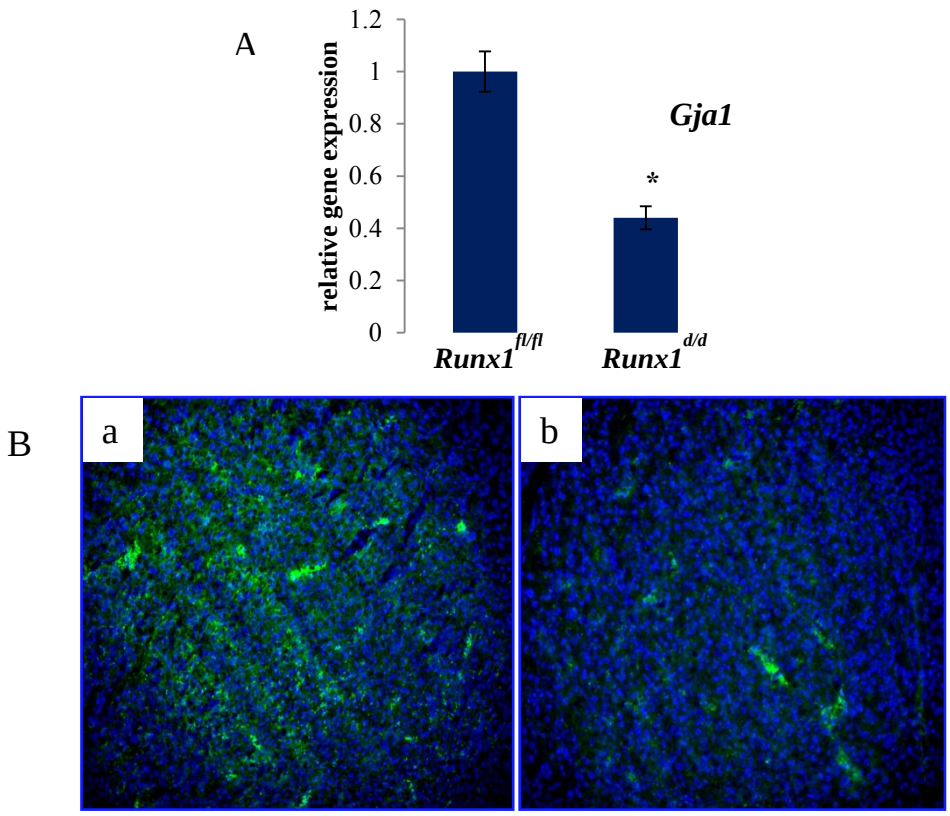

Fig. 15 Down regulation of *Gja1* in *Runx1*$^{d/d}$ uteri

Quantitative PCR of *Gja1* mRNA in day9 pregnant uteri (A). *p< 0.0001
Localization of Gja1 protein in day 9 pregnant uterine sections of *Runx1*$^{fl/fl}$ (B-a) and *Runx1*$^{d/d}$ (B-b) mice.

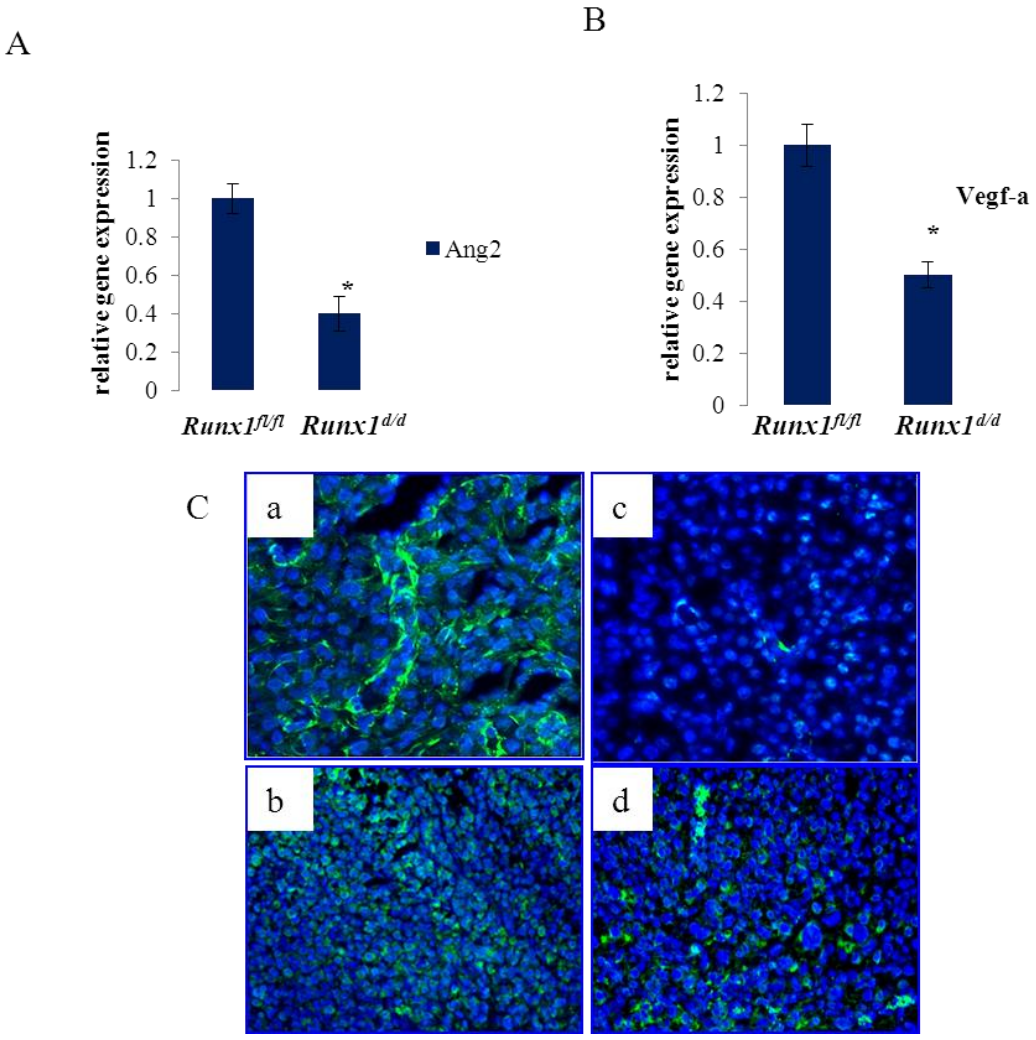

Figure 16. Reduced expression of angiogenic factors in *Runx1*$^{d/d}$ uteri

Quantitative PCR of angiopoietin 2 (A) and Vegf-A (B) in day 9 pregnant uteri (n=5), * $p < 0.001$

Immunolocalization of angiopoietin2 in day 9 uterine sections of Runx1$^{fl/fl}$ (a) and Runx1$^{d/d}$ (c), and Vegf-A in *Runx1*$^{fl/fl}$ (b) and *Runx1*$^{d/d}$ (d).

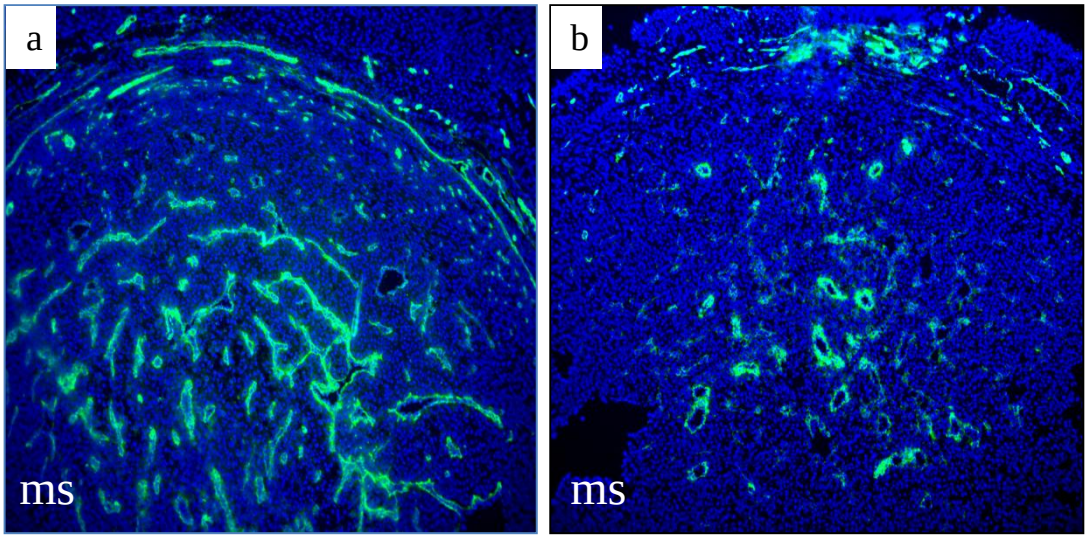

Fig. 17 Impaired angiogenesis in *Runx1*$^{d/d}$ pregnant uteri

Localization of PECAM on day10 pregnant uteri of *Runx1*$^{fl/fl}$ (a) and *Runx1*$^{d/d}$ (b) ms: mesometrium.

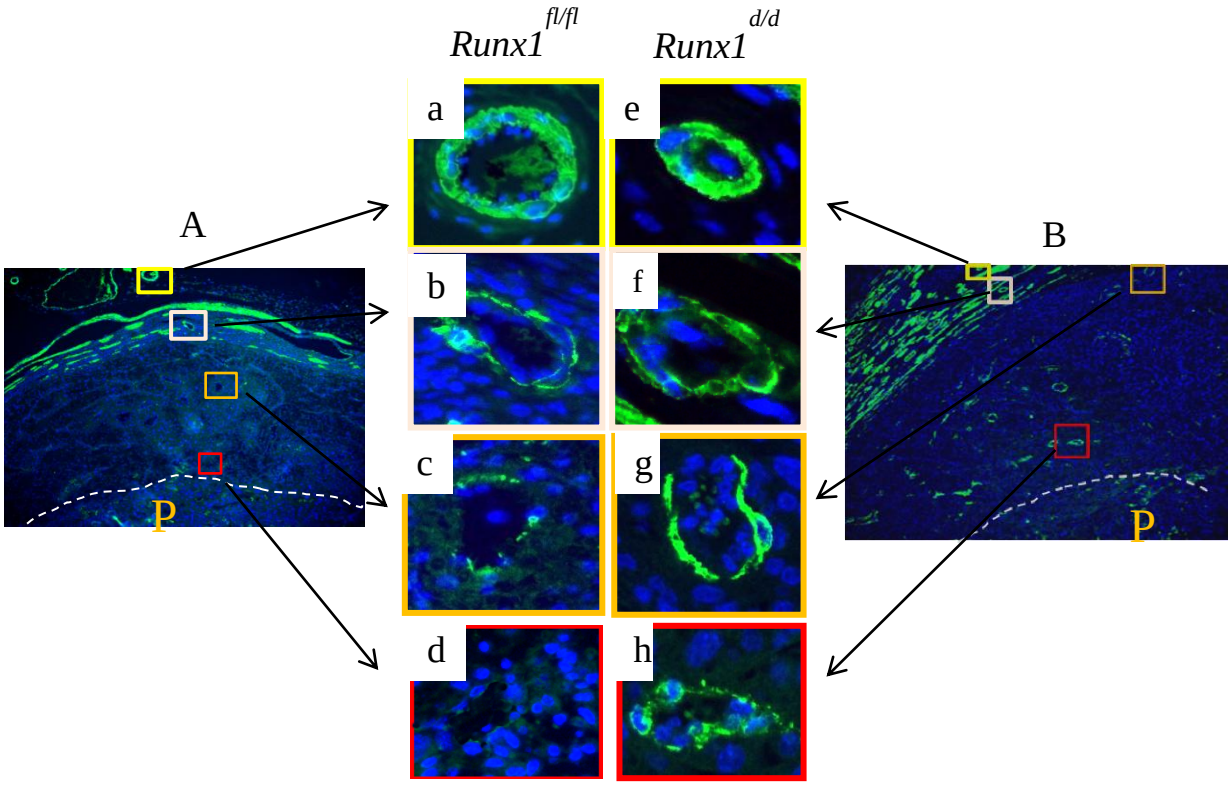

Fig. 18 Spiral artery modification is impaired in *Runx1* null decidua

Localization of α-SMA on day 12 *Runx1*$^{fl/fl}$ (Aa--d) and *Runx1*$^{d/d}$ (Be-h) uterine sections, a&e are radial arteries of *Runx1*$^{fl/fl}$ and *Runx1*$^{d/d}$,b &f are spiral arteries in myometrium, c& g are in distal endometrium and d& h are in proximal endometrium. P: placenta. Dotted lines separate maternal decidua from placental labyrinth.

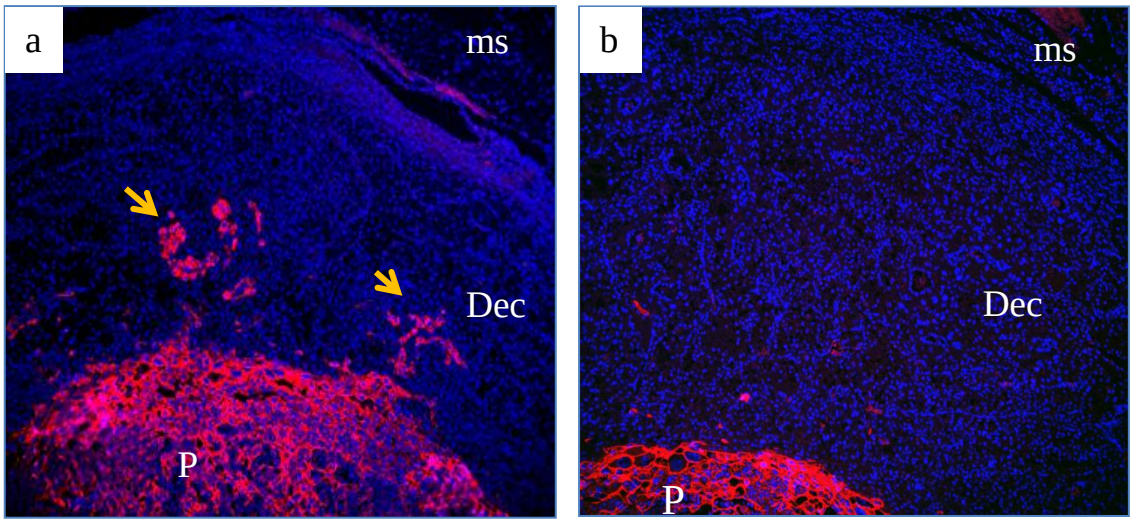

Fig. 19 Impaired trophoblast migration in *Runx1*$^{d/d}$ decidua

Localization of cytokeratin 8 (Troma 1) in day12 *Runx1* $^{fl/fl}$ (a) and *Runx1* $^{d/d}$ (b) uterine sections.
P: placenta, Dec: decidua and ms: mesometrium. Arrows indicate invading fetal trophoblast cells.

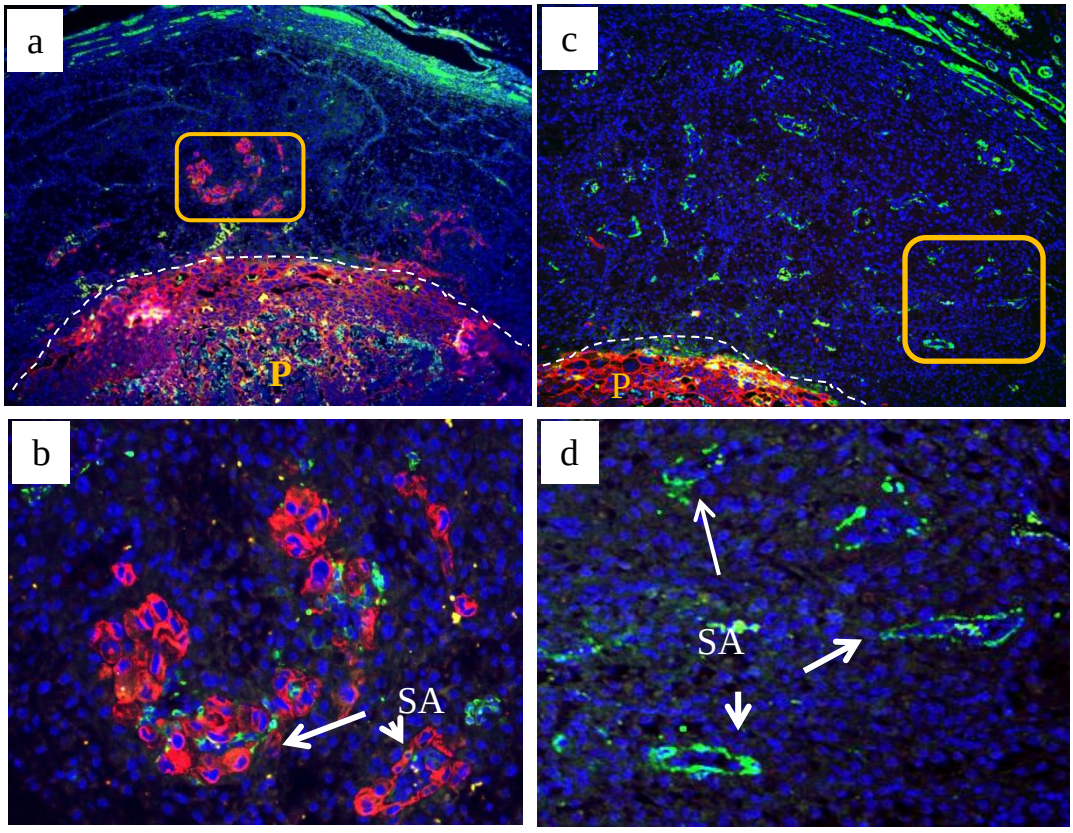

Fig. 20 Maternal-Fetal contact is compromised in *Runx1*$^{d/d}$ decidua

Colocalization of cytokeratin 8 (cy3) and αSMA (FITC) proteins in d12 *Runx1*$^{fl/fl}$ (a& b) and *Runx1*$^{d/d}$ (c & d) uterine sections. b & d are 20x magnification of boxed regions of control and *Runx1*$^{d/d}$ sections.
SA: spiral artery indicated by arrow. P: placenta. Dotted lines separate maternal decidua from placenta.

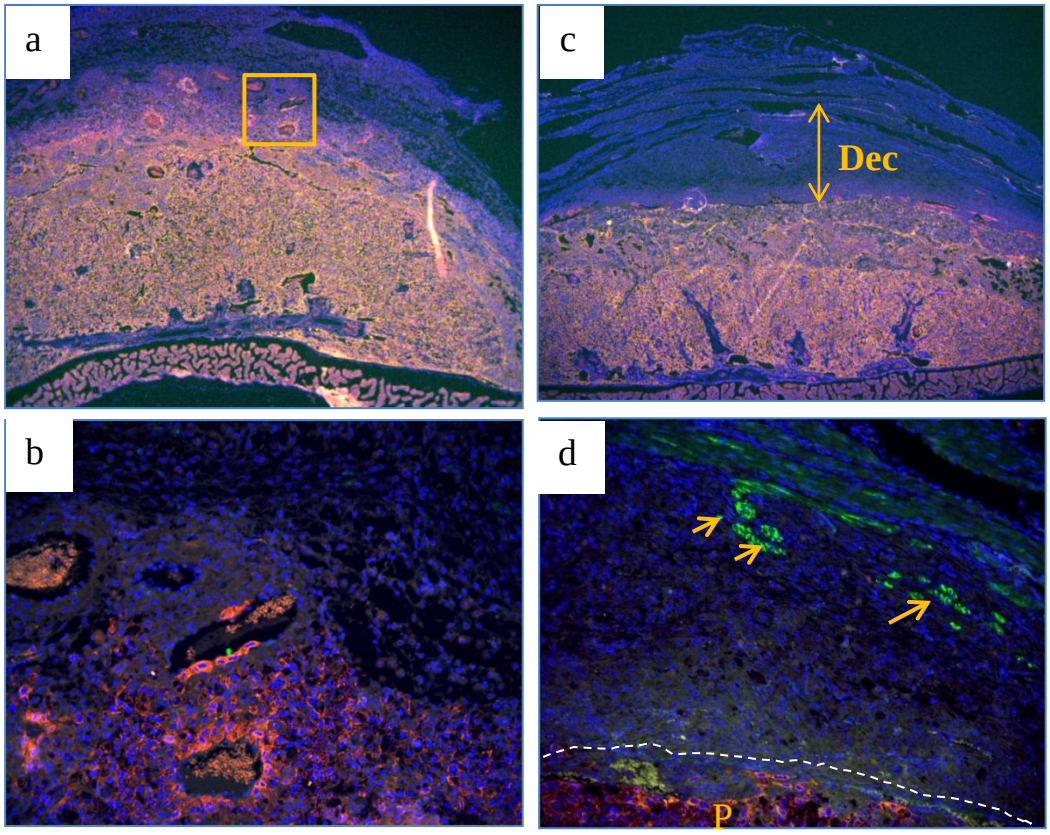

Fig. 21 Compromised trophoblast migration in day 15 *Runx1*$^{d/d}$ decidua

Colocalization of cytokeratin8 (cy3) and αSMA (FITC) in day15 pregnant *Runx1*$^{fl/fl}$ (a & b) and *Runx1*$^{d/d}$ (c & d)
20x magnification of boxed area in *Runx1*$^{fl/fl}$ (b) and *Runx1*$^{d/d}$ (d) decidua. Arrow indicates αSMA positive distal spiral arteries in *Runx1*$^{d/d}$ decidua (d).
Dec: decidua, P: placenta.

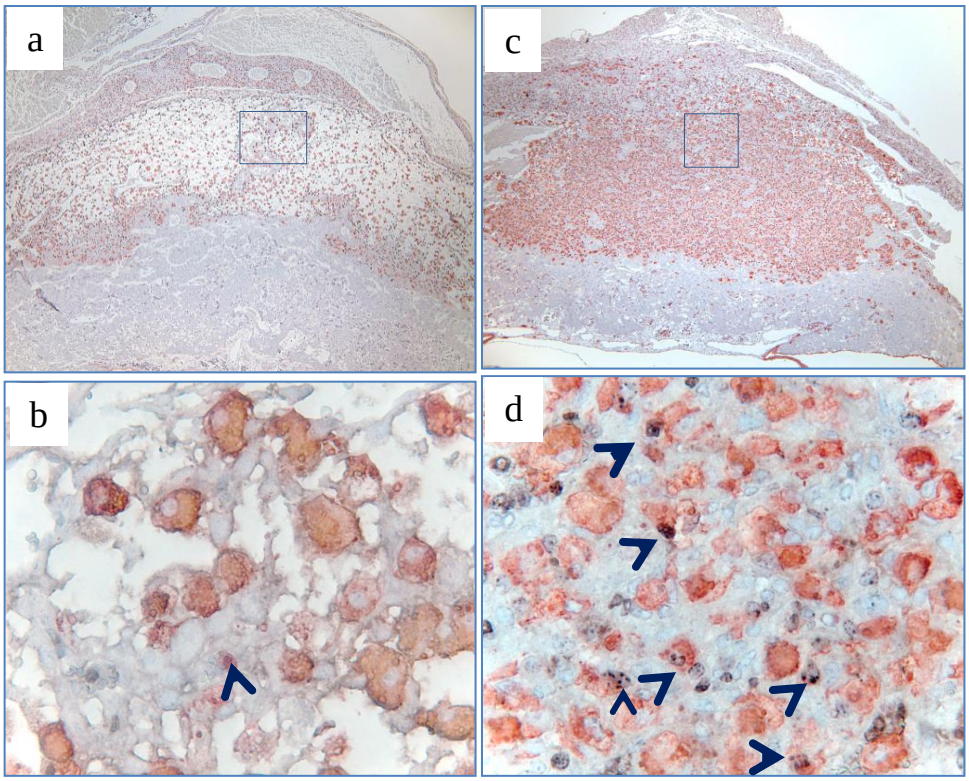

Fig. 22 Increased uNK cell population in *Runx1*$^{d/d}$ decidua

Colocalization of DBA (red) and Ki67 (black) in day12 uterine sections of *Runx1*$^{fl/fl}$ (a & b) and *Runx1*$^{d/d}$ (fig c &d). Colocalized Ki67 positive proliferating uNK cells are indicated by arrow heads.
40x magnification of boxed area of a & c were shown in *Runx1*$^{fl/fl}$ (b) and *Runx1*$^{d/d}$ (d).

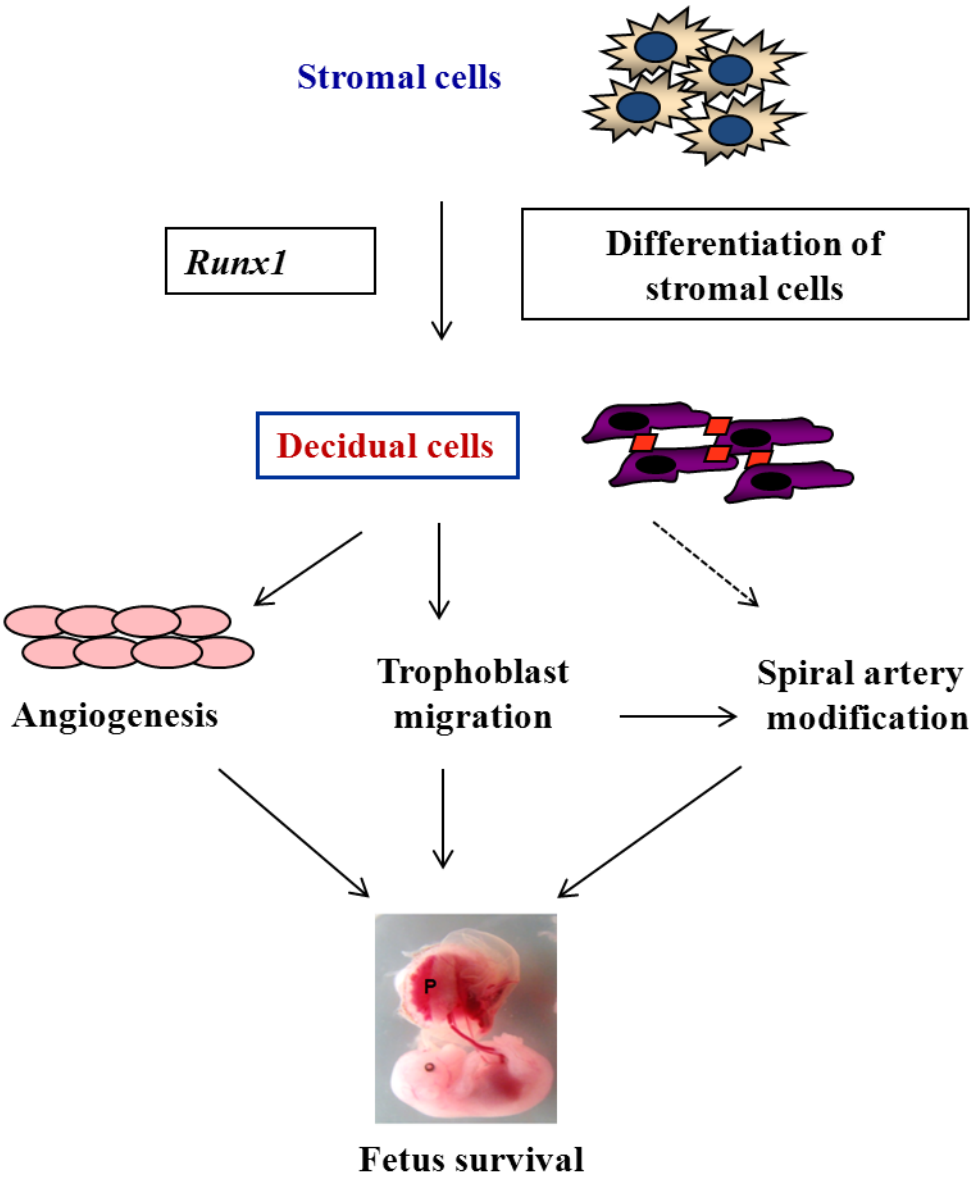

Fig. 23 Summary on the role of *Runx1* during pregnancy

REFERENCES

1. Finn, C. A., and Martin, L. (1974) The control of implantation. *J Reprod Fertil* **39**, 195-206
2. Psychoyos, A. (ed) (1973) *Endocrine control of egg implantation*, Vol. American Physiological Society, Washington, DC
3. Yoshinaga, K. (1988) Uterine receptivity for blastocyst implantation. *Ann N Y Acad Sci* **541**, 424-431
4. Adamson, S. L., Lu, Y., Whiteley, K. J., Holmyard, D., Hemberger, M., Pfarrer, C., and Cross, J. C. (2002) Interactions between trophoblast cells and the maternal and fetal circulation in the mouse placenta. *Dev Biol* **250**, 358-373
5. Cross, J. C., Coan, P. M., Fundele, R., Hemberger, M., Kibschull, M., and Ferguson-Smith, A. (2004) Genes and development--a workshop report. *Placenta* **25 Suppl A**, S39-41
6. Cross, J. C., Hemberger, M., Lu, Y., Nozaki, T., Whiteley, K., Masutani, M., and Adamson, S. L. (2002) Trophoblast functions, angiogenesis and remodeling of the maternal vasculature in the placenta. *Mol Cell Endocrinol* **187**, 207-212
7. Cross, J. C., Werb, Z., and Fisher, S. J. (1994) Implantation and the placenta: key pieces of the development puzzle. *Science* **266**, 1508-1518
8. Carson, D. D., Bagchi, I., Dey, S. K., Enders, A. C., Fazleabas, A. T., Lessey, B. A., and Yoshinaga, K. (2000) Embryo implantation. *Dev Biol* **223**, 217-237
9. Lee, K. Y., and DeMayo, F. J. (2004) Animal models of implantation. *Reproduction* **128**, 679-695
10. Lee, K. Y., Jeong, J. W., Tsai, S. Y., Lydon, J. P., and DeMayo, F. J. (2007) Mouse models of implantation. *Trends Endocrinol Metab* **18**, 234-239
11. Conneely, O. M., Mulac-Jericevic, B., DeMayo, F., Lydon, J. P., and O'Malley, B. W. (2002) Reproductive functions of progesterone receptors. *Recent Prog Horm Res* **57**, 339-355
12. Huet, Y. M., and Dey, S. K. (1987) Role of early and late oestrogenic effects on implantation in the mouse. *J Reprod Fertil* **81**, 453-458
13. Psychoyos, A. (ed) (1973) *Handbook of physiology*, Am. Physiol. Soc, Washington D.C
14. Psychoyos, A. (ed) (1995) *Nidation window*, Springer, New York
15. Yoshinaga, K., and Adams, C. E. (1966) Delayed implantation in the spayed, progesterone treated adult mouse. *J Reprod Fertil* **12**, 593-595
16. Kennedy, T. G. (2003) Decidualization. in *Encyclopedia of Hormones* (Editors-in-Chief: Helen, L. H., and Anthony, W. N. eds.), Academic Press, New York. pp 379-385
17. Gellersen, B., Brosens, I. A., and Brosens, J. J. (2007) Decidualization of the human endometrium: mechanisms, functions, and clinical perspectives. *Semin Reprod Med* **25**, 445-453
18. Ramathal, C. Y., Bagchi, I. C., Taylor, R. N., and Bagchi, M. K. (2010) Endometrial decidualization: of mice and men. *Semin Reprod Med* **28**, 17-26
19. Sapin, V., Blanchon, L., Serre, A. F., Lemery, D., Dastugue, B., and Ward, S. J. (2001) Use of transgenic mice model for understanding the placentation: towards clinical applications in human obstetrical pathologies? *Transgenic research* **10**, 377-398
20. Bagchi, I. C., Li, Q., and Cheon, Y. P. (2001) Role of steroid hormone-regulated genes in implantation. *Ann N Y Acad Sci* **943**, 68-76
21. Psychoyos, A. (1986) Uterine receptivity for nidation. *Ann N Y Acad Sci* **476**, 36-42

22. Weitlauf, H. M. (ed) (1994) *Biology of implantation*, Raven Press, New York
23. Parr, M. B. E. L. P. (ed) (1989) *The implantation reaction*, Plenum Press, New York
24. Dey, S. K., Lim, H., Das, S. K., Reese, J., Paria, B. C., Daikoku, T., and Wang, H. (2004) Molecular cues to implantation. *Endocr Rev* **25**, 341-373
25. Finn, C. A. (1977) The Implantation Reaction. in *Biology of the Uterus* (Wynn, R. M. ed.), Plenum Press, New York. pp 246-308
26. Chakraborty, I., Das, S. K., and Dey, S. K. (1995) Differential expression of vascular endothelial growth factor and its receptor mRNAs in the mouse uterus around the time of implantation. *J Endocrinol* **147**, 339-352
27. Hyder, S. M., and Stancel, G. M. (1999) Regulation of angiogenic growth factors in the female reproductive tract by estrogens and progestins. *Mol Endocrinol* **13**, 806-811
28. Halder, J. B., Zhao, X., Soker, S., Paria, B. C., Klagsbrun, M., Das, S. K., and Dey, S. K. (2000) Differential expression of VEGF isoforms and VEGF(164)-specific receptor neuropilin-1 in the mouse uterus suggests a role for VEGF(164) in vascular permeability and angiogenesis during implantation. *Genesis* **26**, 213-224
29. Geusens, N., Hering, L., Verlohren, S., Luyten, C., Drijkoningen, K., Taube, M., Vercruysse, L., Hanssens, M., Dechend, R., and Pijnenborg, R. (2010) Changes in endovascular trophoblast invasion and spiral artery remodelling at term in a transgenic preeclamptic rat model. *Placenta* **31**, 320-326
30. Kaufmann, P., Black, S., and Huppertz, B. (2003) Endovascular trophoblast invasion: implications for the pathogenesis of intrauterine growth retardation and preeclampsia. *Biol Reprod* **69**, 1-7
31. Ferrara, N., and Davis-Smyth, T. (1997) The biology of vascular endothelial growth factor. *Endocr Rev* **18**, 4-25
32. Carmeliet, P., Ferreira, V., Breier, G., Pollefeyt, S., Kieckens, L., Gertsenstein, M., Fahrig, M., Vandenhoeck, A., Harpal, K., Eberhardt, C., Declercq, C., Pawling, J., Moons, L., Collen, D., Risau, W., and Nagy, A. (1996) Abnormal blood vessel development and lethality in embryos lacking a single VEGF allele. *Nature* **380**, 435-439
33. Ferrara, N., Carver-Moore, K., Chen, H., Dowd, M., Lu, L., O'Shea, K. S., Powell-Braxton, L., Hillan, K. J., and Moore, M. W. (1996) Heterozygous embryonic lethality induced by targeted inactivation of the VEGF gene. *Nature* **380**, 439-442
34. Wulff, C., Wilson, H., Dickson, S. E., Wiegand, S. J., and Fraser, H. M. (2002) Hemochorial placentation in the primate: expression of vascular endothelial growth factor, angiopoietins, and their receptors throughout pregnancy. *Biol Reprod* **66**, 802-812
35. Yu, Q., and Stamenkovic, I. (2001) Angiopoietin-2 is implicated in the regulation of tumor angiogenesis. *Am J Pathol* **158**, 563-570
36. Ma, W., Tan, J., Matsumoto, H., Robert, B., Abrahamson, D. R., Das, S. K., and Dey, S. K. (2001) Adult tissue angiogenesis: evidence for negative regulation by estrogen in the uterus. *Mol Endocrinol* **15**, 1983-1992
37. Walter, L. M., Rogers, P. A., and Girling, J. E. (2005) The role of progesterone in endometrial angiogenesis in pregnant and ovariectomised mice. *Reproduction* **129**, 765-777
38. Aubuchon, M., Schulz, L. C., and Schust, D. J. (2011) Preeclampsia: animal models for a human cure. *Proc Natl Acad Sci U S A* **108**, 1197-1198
39. Coan, P. M., Ferguson-Smith, A. C., and Burton, G. J. (2004) Developmental dynamics of the definitive mouse placenta assessed by stereology. *Biol Reprod* **70**, 1806-1813

40. Rossant, J., and Cross, J. C. (2001) Placental development: lessons from mouse mutants. *Nat Rev Genet* **2**, 538-548
41. Fonseca, B. M., Correia-da-Silva, G., and Teixeira, N. A. (2012) The rat as an animal model for fetoplacental development: a reappraisal of the post-implantation period. *Reprod Biol* **12**, 97-118
42. Brosens, I., Robertson, W. B., and Dixon, H. G. (1967) The physiological response of the vessels of the placental bed to normal pregnancy. *J Pathol Bacteriol* **93**, 569-579
43. Craven, C. M., Morgan, T., and Ward, K. (1998) Decidual spiral artery remodelling begins before cellular interaction with cytotrophoblasts. *Placenta* **19**, 241-252
44. Hirano, H., Imai, Y., and Ito, H. (2002) Spiral artery of placenta: development and pathology-immunohistochemical, microscopical, and electron-microscopic study. *Kobe J Med Sci* **48**, 13-23
45. Pijnenborg, R., Bland, J. M., Robertson, W. B., and Brosens, I. (1983) Uteroplacental arterial changes related to interstitial trophoblast migration in early human pregnancy. *Placenta* **4**, 397-413
46. Kam, E. P., Gardner, L., Loke, Y. W., and King, A. (1999) The role of trophoblast in the physiological change in decidual spiral arteries. *Hum Reprod* **14**, 2131-2138
47. Benirschke K, K. P., and ;. (eds). (2000) *Pathology of the Human Placenta*, Springer, New York
48. Dokras, A., Hoffmann, D. S., Eastvold, J. S., Kienzle, M. F., Gruman, L. M., Kirby, P. A., Weiss, R. M., and Davisson, R. L. (2006) Severe feto-placental abnormalities precede the onset of hypertension and proteinuria in a mouse model of preeclampsia. *Biol Reprod* **75**, 899-907
49. Rasmussen, S., and Irgens, L. M. (2003) Fetal growth and body proportion in preeclampsia. *Obstet Gynecol* **101**, 575-583
50. Long, P. A., Abell, D. A., and Beischer, N. A. (1980) Fetal growth retardation and pre-eclampsia. *Br J Obstet Gynaecol* **87**, 13-18
51. Lim, H. J., and Wang, H. (2010) Uterine disorders and pregnancy complications: insights from mouse models. *J Clin Invest* **120**, 1004-1015
52. Kanayama, N., Takahashi, K., Matsuura, T., Sugimura, M., Kobayashi, T., Moniwa, N., Tomita, M., and Nakayama, K. (2002) Deficiency in p57Kip2 expression induces preeclampsia-like symptoms in mice. *Mol Hum Reprod* **8**, 1129-1135
53. Canon, J., and Banerjee, U. (2000) Runt and Lozenge function in Drosophila development. *Semin Cell Dev Biol* **11**, 327-336
54. Ito, Y. (2004) Oncogenic potential of the RUNX gene family: 'overview'. *Oncogene* **23**, 4198-4208
55. van Wijnen, A. J., Stein, G. S., Gergen, J. P., Groner, Y., Hiebert, S. W., Ito, Y., Liu, P., Neil, J. C., Ohki, M., and Speck, N. (2004) Nomenclature for Runt-related (RUNX) proteins. *Oncogene* **23**, 4209-4210
56. Cohen, M. M., Jr. (2001) RUNX genes, neoplasia, and cleidocranial dysplasia. *Am J Med Genet* **104**, 185-188
57. Liu, H., Carlsson, L., and Grundstrom, T. (2006) Identification of an N-terminal transactivation domain of Runx1 that separates molecular function from global differentiation function. *J Biol Chem* **281**, 25659-25669
58. Cohen, M. M., Jr. (2009) Perspectives on RUNX genes: an update. *Am J Med Genet A* **149A**, 2629-2646

59. Miyoshi, H., Shimizu, K., Kozu, T., Maseki, N., Kaneko, Y., and Ohki, M. (1991) t(8;21) breakpoints on chromosome 21 in acute myeloid leukemia are clustered within a limited region of a single gene, AML1. *Proc Natl Acad Sci U S A* **88**, 10431-10434
60. Okuda, T., van Deursen, J., Hiebert, S. W., Grosveld, G., and Downing, J. R. (1996) AML1, the target of multiple chromosomal translocations in human leukemia, is essential for normal fetal liver hematopoiesis. *Cell* **84**, 321-330
61. Tracey, W. D., and Speck, N. A. (2000) Potential roles for RUNX1 and its orthologs in determining hematopoietic cell fate. *Semin Cell Dev Biol* **11**, 337-342
62. Levanon, D., and Groner, Y. (2004) Structure and regulated expression of mammalian RUNX genes. *Oncogene* **23**, 4211-4219
63. Woolf, E., Xiao, C., Fainaru, O., Lotem, J., Rosen, D., Negreanu, V., Bernstein, Y., Goldenberg, D., Brenner, O., Berke, G., Levanon, D., and Groner, Y. (2003) Runx3 and Runx1 are required for CD8 T cell development during thymopoiesis. *Proc Natl Acad Sci U S A* **100**, 7731-7736
64. Yamashiro, T., Aberg, T., Levanon, D., Groner, Y., and Thesleff, I. (2002) Expression of Runx1, -2 and -3 during tooth, palate and craniofacial bone development. *Gene Expr Patterns* **2**, 109-112
65. Yamashiro, T., Wang, X. P., Li, Z., Oya, S., Aberg, T., Fukunaga, T., Kamioka, H., Speck, N. A., Takano-Yamamoto, T., and Thesleff, I. (2004) Possible roles of Runx1 and Sox9 in incipient intramembranous ossification. *J Bone Miner Res* **19**, 1671-1677
66. Levanon, D., Brenner, O., Negreanu, V., Bettoun, D., Woolf, E., Eilam, R., Lotem, J., Gat, U., Otto, F., Speck, N., and Groner, Y. (2001) Spatial and temporal expression pattern of Runx3 (Aml2) and Runx1 (Aml1) indicates non-redundant functions during mouse embryogenesis. *Mech Dev* **109**, 413-417
67. Jeong, J. H., Jin, J. S., Kim, H. N., Kang, S. M., Liu, J. C., Lengner, C. J., Otto, F., Mundlos, S., Stein, J. L., van Wijnen, A. J., Lian, J. B., Stein, G. S., and Choi, J. Y. (2008) Expression of Runx2 transcription factor in non-skeletal tissues, sperm and brain. *J Cell Physiol* **217**, 511-517
68. McRae, R. S., Johnston, H. M., Mihm, M., and O'Shaughnessy, P. J. (2005) Changes in mouse granulosa cell gene expression during early luteinization. *Endocrinology* **146**, 309-317
69. Sakuma, A., Fukamachi, H., Ito, K., Ito, Y., Takeuchi, S., and Takahashi, S. (2008) Loss of Runx3 affects ovulation and estrogen-induced endometrial cell proliferation in female mice. *Mol Reprod Dev* **75**, 1653-1661
70. Jo, M., and Curry, T. E., Jr. (2006) Luteinizing hormone-induced RUNX1 regulates the expression of genes in granulosa cells of rat periovulatory follicles. *Mol Endocrinol* **20**, 2156-2172
71. Liu, J., Park, E. S., Curry, T. E., Jr., and Jo, M. (2010) Periovulatory expression of hyaluronan and proteoglycan link protein 1 (Hapln1) in the rat ovary: hormonal regulation and potential function. *Mol Endocrinol* **24**, 1203-1217
72. Park, E. S., Lind, A. K., Dahm-Kahler, P., Brannstrom, M., Carletti, M. Z., Christenson, L. K., Curry, T. E., Jr., and Jo, M. (2010) RUNX2 transcription factor regulates gene expression in luteinizing granulosa cells of rat ovaries. *Mol Endocrinol* **24**, 846-858
73. Doll, A., Gonzalez, M., Abal, M., Llaurado, M., Rigau, M., Colas, E., Monge, M., Xercavins, J., Capella, G., Diaz, B., Gil-Moreno, A., Alameda, F., and Reventos, J.

(2009) An orthotopic endometrial cancer mouse model demonstrates a role for RUNX1 in distant metastasis. *Int J Cancer* **125**, 257-263

74. Planaguma, J., Diaz-Fuertes, M., Gil-Moreno, A., Abal, M., Monge, M., Garcia, A., Baro, T., Thomson, T. M., Xercavins, J., Alameda, F., and Reventos, J. (2004) A differential gene expression profile reveals overexpression of RUNX1/AML1 in invasive endometrioid carcinoma. *Cancer Res* **64**, 8846-8853
75. Growney, J. D., Shigematsu, H., Li, Z., Lee, B. H., Adelsperger, J., Rowan, R., Curley, D. P., Kutok, J. L., Akashi, K., Williams, I. R., Speck, N. A., and Gilliland, D. G. (2005) Loss of Runx1 perturbs adult hematopoiesis and is associated with a myeloproliferative phenotype. *Blood* **106**, 494-504
76. Soyal, S. M., Mukherjee, A., Lee, K. Y., Li, J., Li, H., DeMayo, F. J., and Lydon, J. P. (2005) Cre-mediated recombination in cell lineages that express the progesterone receptor. *Genesis* **41**, 58-66
77. DeLisser, H. M., Christofidou-Solomidou, M., Strieter, R. M., Burdick, M. D., Robinson, C. S., Wexler, R. S., Kerr, J. S., Garlanda, C., Merwin, J. R., Madri, J. A., and Albelda, S. M. (1997) Involvement of endothelial PECAM-1/CD31 in angiogenesis. *Am J Pathol* **151**, 671-677
78. Lydon, J. P., DeMayo, F. J., Funk, C. R., Mani, S. K., Hughes, A. R., Montgomery, C. A., Jr., Shyamala, G., Conneely, O. M., and O'Malley, B. W. (1995) Mice lacking progesterone receptor exhibit pleiotropic reproductive abnormalities. *Genes Dev* **9**, 2266-2278
79. Kannan, A., Fazleabas, A. T., Bagchi, I. C., and Bagchi, M. K. (2010) The transcription factor C/EBPbeta is a marker of uterine receptivity and expressed at the implantation site in the primate. *Reprod Sci* **17**, 434-443
80. Li, Q., Kannan, A., Wang, W., Demayo, F. J., Taylor, R. N., Bagchi, M. K., and Bagchi, I. C. (2007) Bone morphogenetic protein 2 functions via a conserved signaling pathway involving Wnt4 to regulate uterine decidualization in the mouse and the human. *J Biol Chem* **282**, 31725-31732
81. Das, A., Li, Q., Laws, M. J., Kaya, H., Bagchi, M. K., and Bagchi, I. C. (2012) Estrogen-induced expression of Fos-related antigen 1 (FRA-1) regulates uterine stromal differentiation and remodeling. *J Biol Chem* **287**, 19622-19630
82. Livak, K. J., and Schmittgen, T. D. (2001) Analysis of relative gene expression data using real-time quantitative PCR and the 2(-Delta Delta C(T)) Method. *Methods* **25**, 402-408
83. Gupta, R. K., Meachum, S., Hernandez-Ochoa, I., Peretz, J., Yao, H. H., and Flaws, J. A. (2009) Methoxychlor inhibits growth of antral follicles by altering cell cycle regulators. *Toxicol Appl Pharmacol* **240**, 1-7
84. Hernandez-Ochoa, I., Barnett-Ringgold, K. R., Dehlinger, S. L., Gupta, R. K., Leslie, T. C., Roby, K. F., and Flaws, J. A. (2010) The ability of the aryl hydrocarbon receptor to regulate ovarian follicle growth and estradiol biosynthesis in mice depends on stage of sexual maturity. *Biol Reprod* **83**, 698-706
85. Gidley-Baird, A. A. (1981) Endocrine control of implantation and delayed implantation in rats and mice. *J Reprod Fertil Suppl* **29**, 97-109
86. Wang, Q., Stacy, T., Binder, M., Marin-Padilla, M., Sharpe, A. H., and Speck, N. A. (1996) Disruption of the Cbfa2 gene causes necrosis and hemorrhaging in the central

nervous system and blocks definitive hematopoiesis. *Proc Natl Acad Sci U S A* **93**, 3444-3449

87. Kurihara, I., Lee, D. K., Petit, F. G., Jeong, J., Lee, K., Lydon, J. P., DeMayo, F. J., Tsai, M. J., and Tsai, S. Y. (2007) COUP-TFII mediates progesterone regulation of uterine implantation by controlling ER activity. *PLoS Genet* **3**, e102
88. Laws, M. J., Taylor, R. N., Sidell, N., DeMayo, F. J., Lydon, J. P., Gutstein, D. E., Bagchi, M. K., and Bagchi, I. C. (2008) Gap junction communication between uterine stromal cells plays a critical role in pregnancy-associated neovascularization and embryo survival. *Development* **135**, 2659-2668
89. Lee, K., Jeong, J., Kwak, I., Yu, C. T., Lanske, B., Soegiarto, D. W., Toftgard, R., Tsai, M. J., Tsai, S., Lydon, J. P., and DeMayo, F. J. (2006) Indian hedgehog is a major mediator of progesterone signaling in the mouse uterus. *Nat Genet* **38**, 1204-1209
90. Mantena, S. R., Kannan, A., Cheon, Y. P., Li, Q., Johnson, P. F., Bagchi, I. C., and Bagchi, M. K. (2006) C/EBPbeta is a critical mediator of steroid hormone-regulated cell proliferation and differentiation in the uterine epithelium and stroma. *Proc Natl Acad Sci U S A* **103**, 1870-1875
91. Roumier, C., Fenaux, P., Lafage, M., Imbert, M., Eclache, V., and Preudhomme, C. (2003) New mechanisms of AML1 gene alteration in hematological malignancies. *Leukemia* **17**, 9-16
92. Takano, M., Lu, Z., Goto, T., Fusi, L., Higham, J., Francis, J., Withey, A., Hardt, J., Cloke, B., Stavropoulou, A. V., Ishihara, O., Lam, E. W., Unterman, T. G., Brosens, J. J., and Kim, J. J. (2007) Transcriptional cross talk between the forkhead transcription factor forkhead box O1A and the progesterone receptor coordinates cell cycle regulation and differentiation in human endometrial stromal cells. *Mol Endocrinol* **21**, 2334-2349
93. Risinger, J. I., Maxwell, G. L., Chandramouli, G. V., Jazaeri, A., Aprelikova, O., Patterson, T., Berchuck, A., and Barrett, J. C. (2003) Microarray analysis reveals distinct gene expression profiles among different histologic types of endometrial cancer. *Cancer Res* **63**, 6-11
94. Shazand, K., Baban, S., Prive, C., Malette, B., Croteau, P., Lagace, M., Racine, J. B., and Hugo, P. (2004) FOXO1 and c-jun transcription factors mRNA are modulated in endometriosis. *Mol Hum Reprod* **10**, 871-877
95. Alam, S. M., Konno, T., Dai, G., Lu, L., Wang, D., Dunmore, J. H., Godwin, A. R., and Soares, M. J. (2007) A uterine decidual cell cytokine ensures pregnancy-dependent adaptations to a physiological stressor. *Development* **134**, 407-415
96. Carroll, V. M., Jeyakumar, M., Carlson, K. E., and Katzenellenbogen, J. A. (2012) Diarylpropionitrile (DPN) enantiomers: synthesis and evaluation of estrogen receptor beta-selective ligands. in *J Med Chem*, 2011/11/30 Ed.
97. Cohick, C. B., Xu, L., and Soares, M. J. (1997) Prolactin-like protein-B: heterologous expression and characterization of placental and decidual species. *J Endocrinol* **152**, 291-302
98. Gu, Y., Soares, M. J., Srivastava, R. K., and Gibori, G. (1994) Expression of decidual prolactin-related protein in the rat decidua. *Endocrinology* **135**, 1422-1427
99. Lin, J., Poole, J., and Linzer, D. I. (1997) Three new members of the mouse prolactin/growth hormone family are homologous to proteins expressed in the rat. *Endocrinology* **138**, 5541-5549

100. Delisser, H. M., Baldwin, H. S., and Albelda, S. M. (1997) Platelet Endothelial Cell Adhesion Molecule 1 (PECAM-1/CD31): A Multifunctional Vascular Cell Adhesion Molecule. *Trends Cardiovasc Med* **7**, 203-210
101. Matsumoto, H., Ma, W. G., Daikoku, T., Zhao, X., Paria, B. C., Das, S. K., Trzaskos, J. M., and Dey, S. K. (2002) Cyclooxygenase-2 differentially directs uterine angiogenesis during implantation in mice. *J Biol Chem* **277**, 29260-29267
102. Cartwright, J. E., Fraser, R., Leslie, K., Wallace, A. E., and James, J. L. (2010) Remodelling at the maternal-fetal interface: relevance to human pregnancy disorders. *Reproduction* **140**, 803-813
103. Pijnenborg, R., Vercruysse, L., and Hanssens, M. (2006) The uterine spiral arteries in human pregnancy: facts and controversies. *Placenta* **27**, 939-958
104. Osol, G., and Mandala, M. (2009) Maternal uterine vascular remodeling during pregnancy. *Physiology (Bethesda)* **24**, 58-71
105. Ashkar, A. A., and Croy, B. A. (2001) Functions of uterine natural killer cells are mediated by interferon gamma production during murine pregnancy. *Semin Immunol* **13**, 235-241
106. Ashkar, A. A., Di Santo, J. P., and Croy, B. A. (2000) Interferon gamma contributes to initiation of uterine vascular modification, decidual integrity, and uterine natural killer cell maturation during normal murine pregnancy. *J Exp Med* **192**, 259-270
107. Croy, B. A., Ashkar, A. A., Minhas, K., and Greenwood, J. D. (2000) Can murine uterine natural killer cells give insights into the pathogenesis of preeclampsia? *J Soc Gynecol Investig* **7**, 12-20
108. Whitley, G. S., and Cartwright, J. E. (2010) Cellular and molecular regulation of spiral artery remodelling: lessons from the cardiovascular field. *Placenta* **31**, 465-474
109. Zhang, J., and Salamonsen, L. A. (1997) Tissue inhibitor of metalloproteinases (TIMP)-1, -2 and -3 in human endometrium during the menstrual cycle. *Mol Hum Reprod* **3**, 735-741
110. Kelly, B. A., Bond, B. C., and Poston, L. (2003) Gestational profile of matrix metalloproteinases in rat uterine artery. *Mol Hum Reprod* **9**, 351-358